***New Journal of Chemistry*** article

# Oxaazamacrocycles incorporating quinoline moiety: synthesis and study of their binding properties towards metal cations

A. S. Abel, A. D. Averin and I. P. Beletskaya

*M.V. Lomonosov Moscow State University, Department of Chemistry, 1-3 Leninskie gory, Moscow, 119991, Russia; e-mail: beletska@org.chem.msu.ru*

## Supporting information

## Table of contents

## 1. Studies of binding metal ions by 5a

1.1 Fluorimetric and UV-vis studies of binding metal ions by **5a**

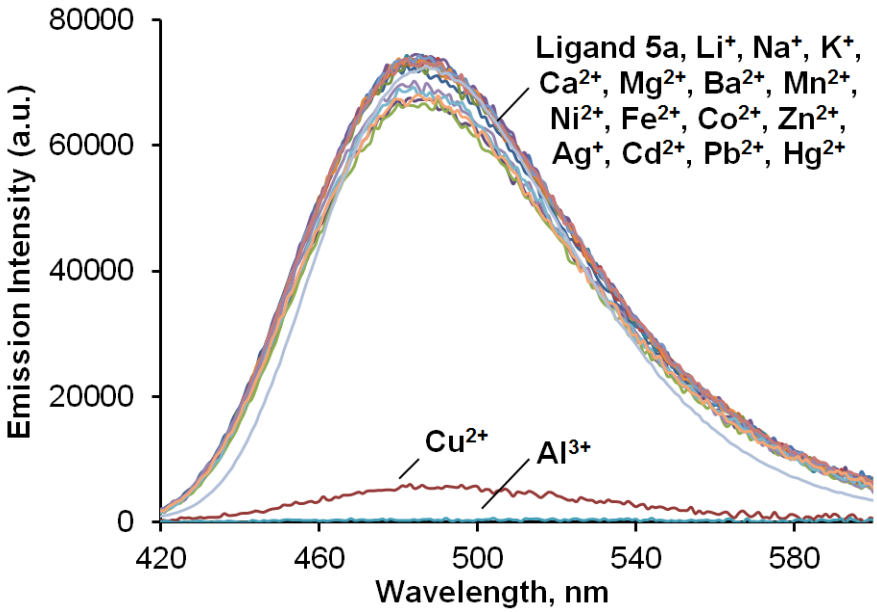


**Figure S1.** Fluorescence spectra of **5a** ([**5a**] = 26 μM) in $CH_3CN$ before and after addition of 4 equiv. of metal perchlorates in $CH_3CN$ ($\lambda_{ex}$ = 397 nm).

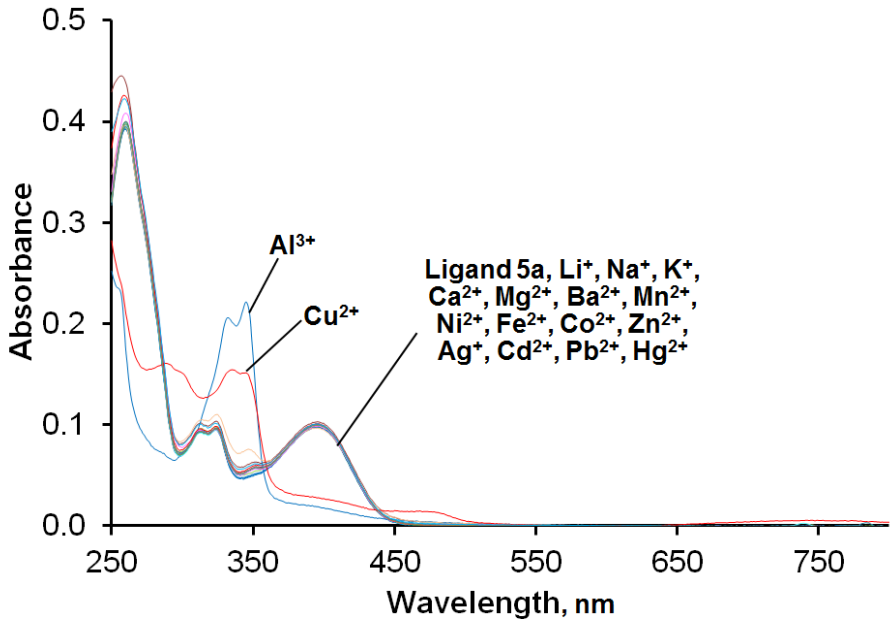


**Figure S2.** UV-vis spectra of **5a** ([**5a**] = 26 μM) in $CH_3CN$ before and after addition of 4 equiv. of metal perchlorates in $CH_3CN$.

1.2 Fluorimetric and spectrophotometric titrations of **5a** with $Cu^{2+}$ ions

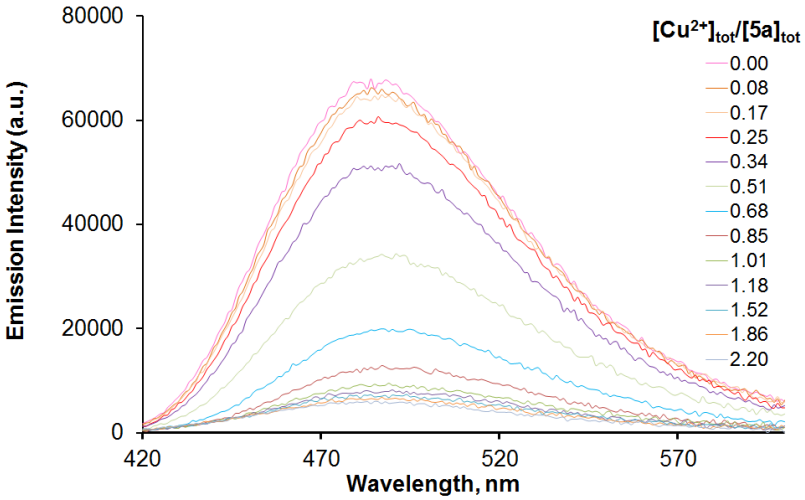


**Figure S3.** Evolution of fluorescence spectrum of **5a** (26 μM solution in $CH_3CN$) upon addition of $Cu(ClO_4)_2$ (0 - 2.2 equiv.) ($\lambda_{ex}$ = 397 nm).

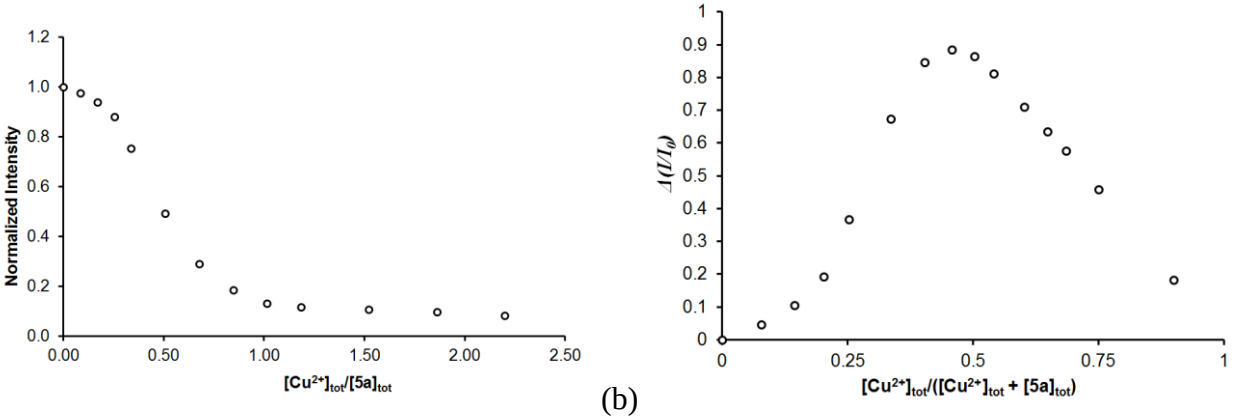


(a) (b)

**Figure S4.** (a) Changes of emission intensities at 488 nm plotted against $[Cu(ClO_4)_2]/[\mathbf{5a}]_{tot}$. (b) Job's plot derived from the titration curve[2].

Stability constants calculated using SPECFIT[1]

$lg(\beta_{Cu(\mathbf{5a})2})$ = 11.7±0.5 , $lg(\beta_{Cu(\mathbf{5a})})$ = 7.0±0.5

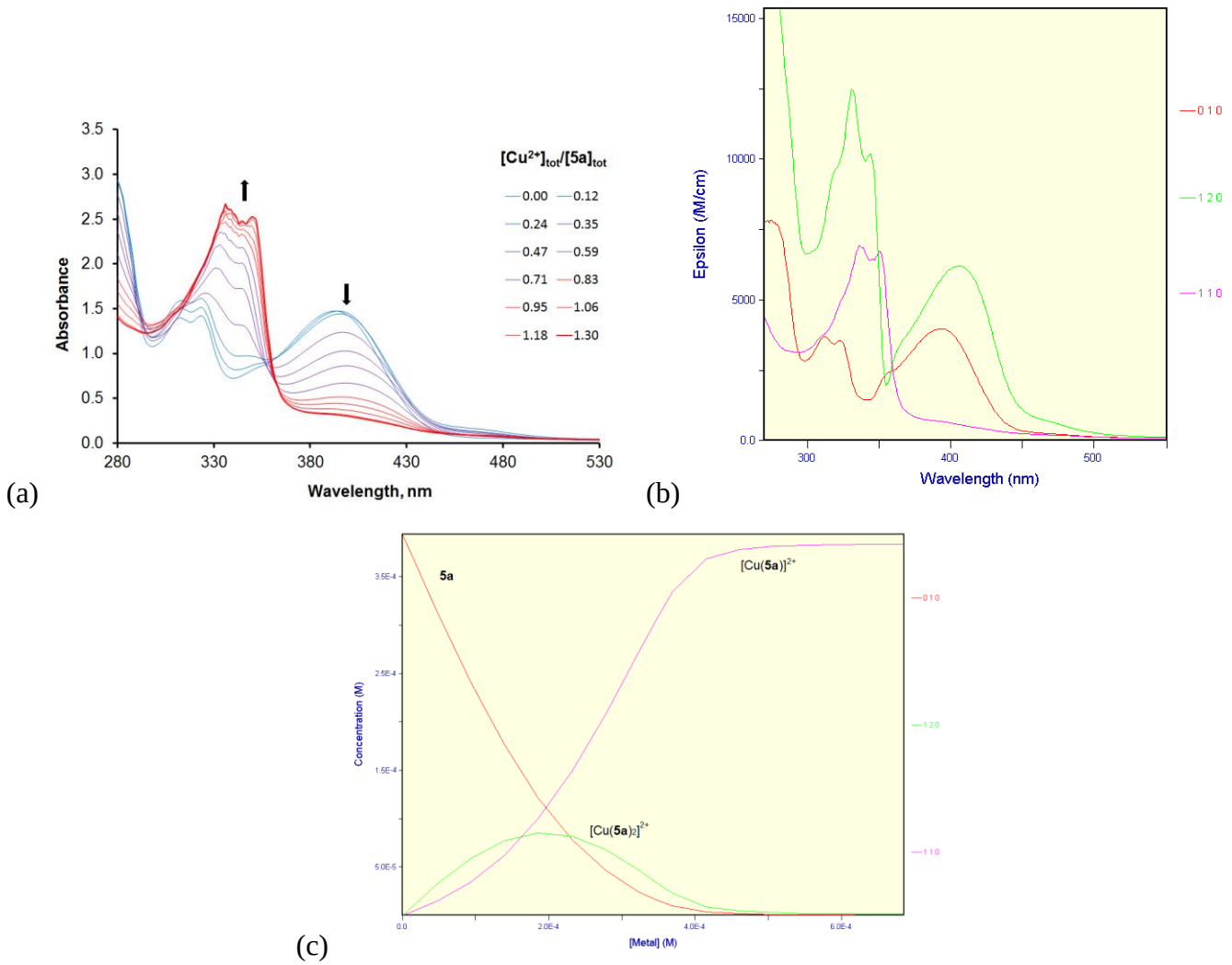


**Figure S5.** (a) Evolution of UV–vis spectrum of **5a** (394 μM solution in $CH_3CN$) upon addition of $Cu(ClO_4)_2$ (0 - 1.3 equiv.). (b) UV-vis spectra of **5a** (red), $[Cu(\mathbf{5a})_2]^{2+}$ (green) and $[Cu(\mathbf{5a})]^{2+}$ (magenta) calculated using SPECFIT[1]. (c) Species distribution diagram for the $Cu^{2+}$/**5a** system in $CH_3CN$ calculated using SPECFIT[1].

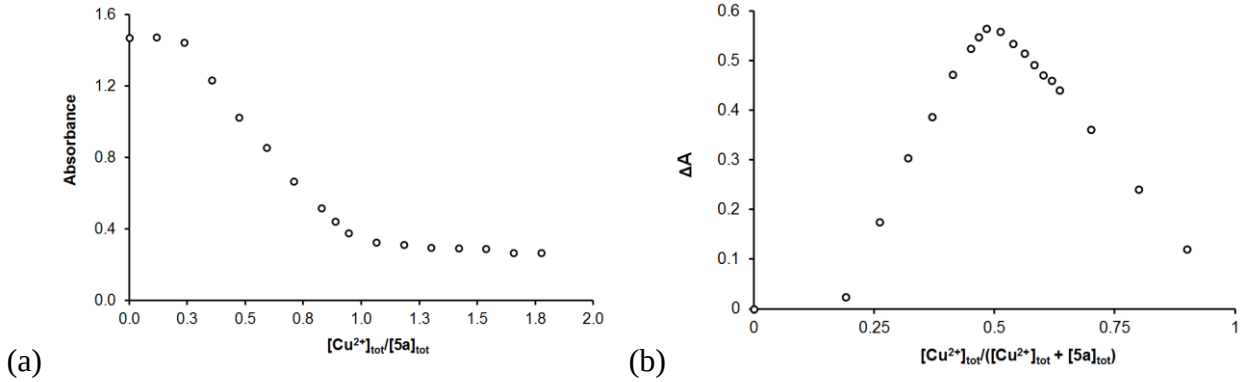


**Figure S6.** (a) Changes of absorbance at 395 nm plotted against $[Cu(ClO_4)_2]/[\mathbf{5a}]_{tot}$. (b) Job's plot derived from the titration curve[2].

Stability constants calculated using SPECFIT[1]

$\lg(\beta_{Cu(\mathbf{5a})2}) = 10.5\pm0.3$ , $\lg(\beta_{Cu(\mathbf{5a})}) = 6.3\pm0.3$

1.3 Fluorimetric and spectrophotometric titrations of **5a** with $Al^{3+}$ ions

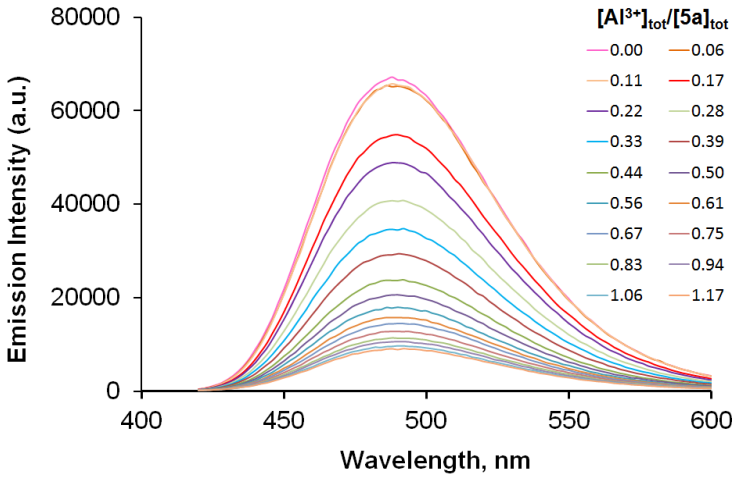


**Figure S7.** Evolution of fluorescence spectrum of **5a** (26 μM solution in $CH_3CN$) upon addition of $Al(ClO_4)_3$ (0 - 1.2 equiv.) ($\lambda_{ex}$ = 397 nm).

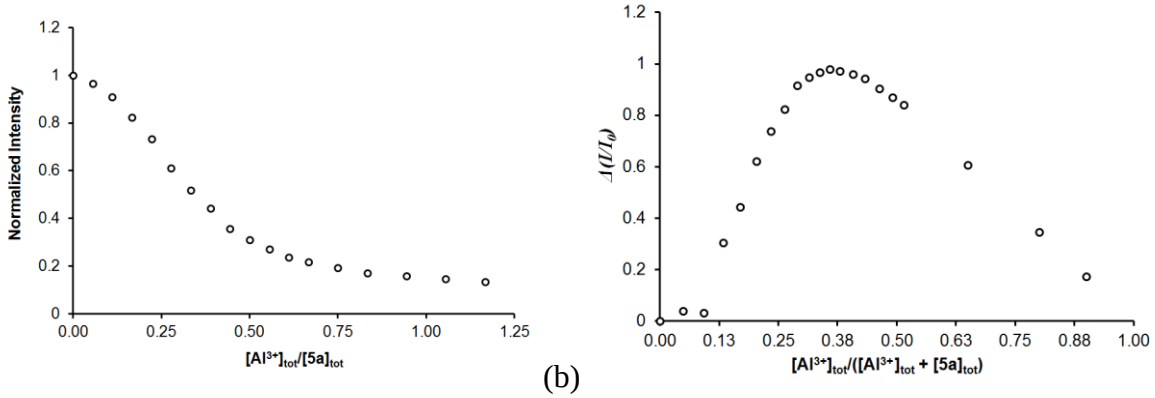


(a) (b)

**Figure S8.** (a) Changes of emission intensities at 488 nm plotted against $[Al(ClO_4)_3]/[\mathbf{5a}]_{tot}$. (b) Job's plot derived from the titration curve[2].

Stability constants calculated using SPECFIT[1]

$lg(\beta_{Al(\mathbf{5a})2})$ = 11.85±0.05

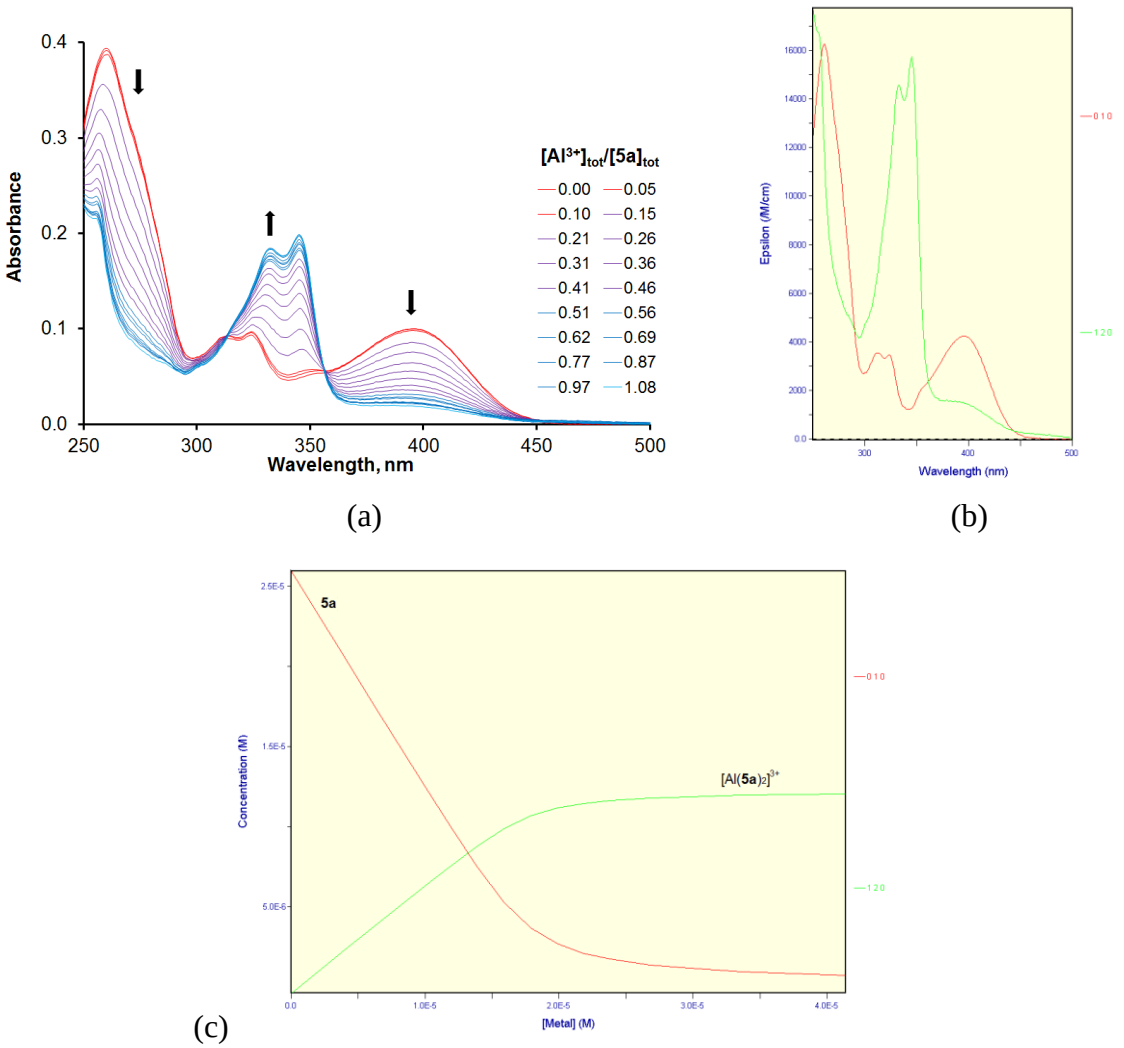


**Figure S9.** (a) Evolution of UV–vis spectrum of **5a** (26 μM solution in $CH_3CN$) upon addition of $Al(ClO_4)_3$ (0 - 1.1 equiv.); (b) Normalized UV-vis spectra of **5a** (red) and $[Al(\mathbf{5a})_2]^{3+}$ (green) calculated using SPECFIT[1]. (c) Species distribution diagram for the $Al^{3+}$/**5a** system in $CH_3CN$ calculated using SPECFIT[1]

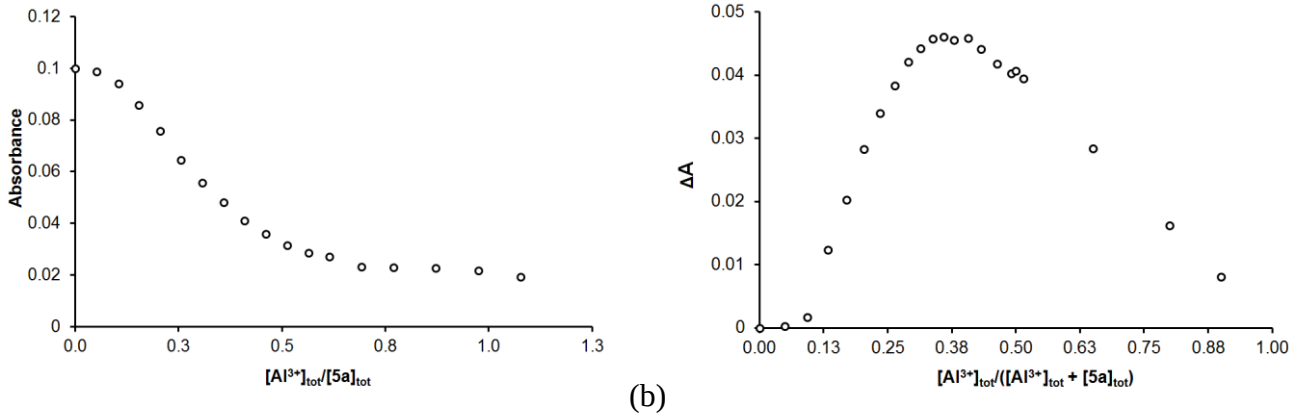


**Figure S10.** (a) Changes of absorbance at 395 nm plotted against $[Al(ClO_4)_3]/[\mathbf{5a}]_{tot}$. (b) Job's plot derived from the titration curve[2].

Stability constants calculated using SPECFIT[1]

$\lg(\beta_{Al(\mathbf{5a})2}) = 11.15 \pm 0.07$

## 2. Studies of binding metal ions by 5b

2.1 Fluorimetric and UV-vis studies of binding metal ions by **5b**

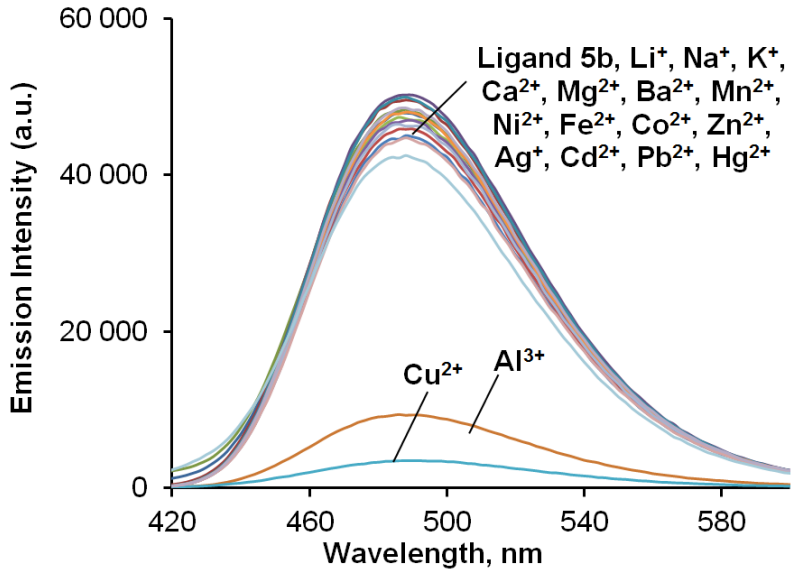


**Figure S11.** Fluorescence spectra of **5b** ([**5b**] = 24 μM) in $CH_3CN$ before and after addition of 4 equiv. of metal perchlorates in $CH_3CN$ ($\lambda_{ex}$ = 395 nm).

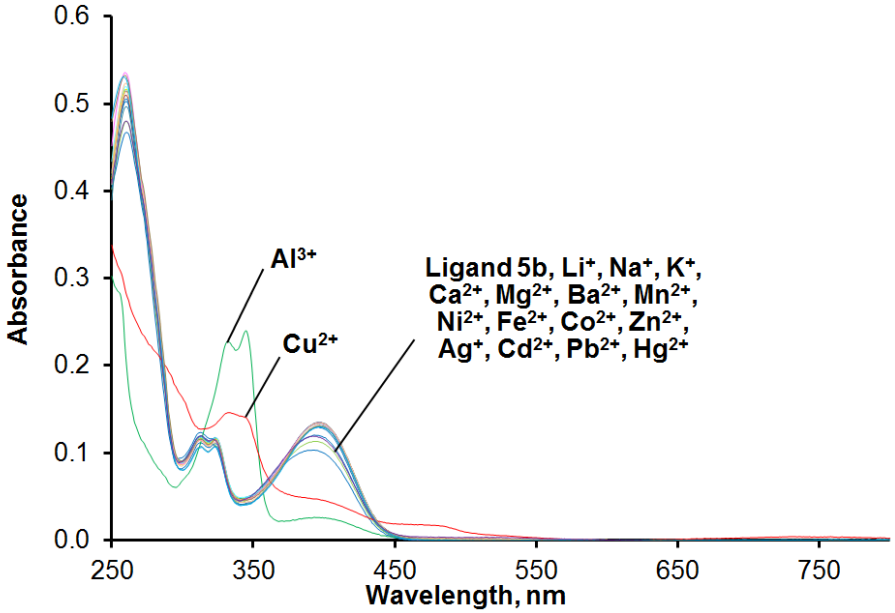


**Figure S12.** UV-vis spectra of **5b** ([**5b**] = 24 μM) in $CH_3CN$ before and after addition of 4 equiv. of metal perchlorates in $CH_3CN$.

## 3. Studies of binding metal ions by 5c

3.1 Fluorimetric and UV-vis studies of binding metal ions by **5c**

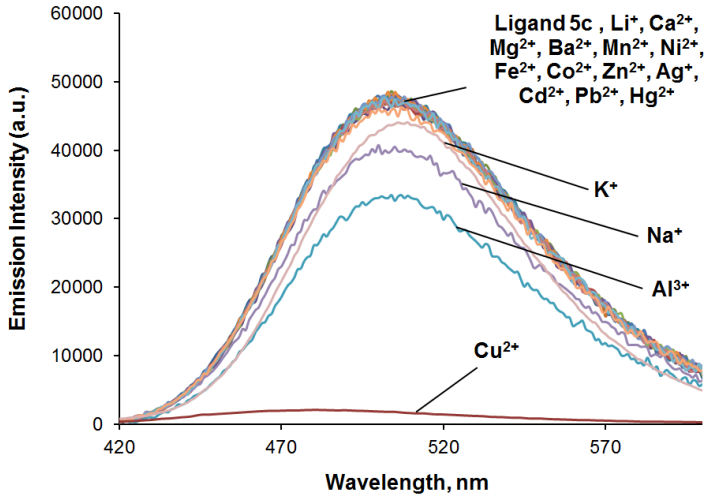


**Figure S13.** Fluorescence spectra of **5c** ([**5c**] = 24 μM) in $CH_3CN$ before and after addition of 4 equiv. of metal perchlorates in $CH_3CN$ ($\lambda_{ex}$ = 385 nm).

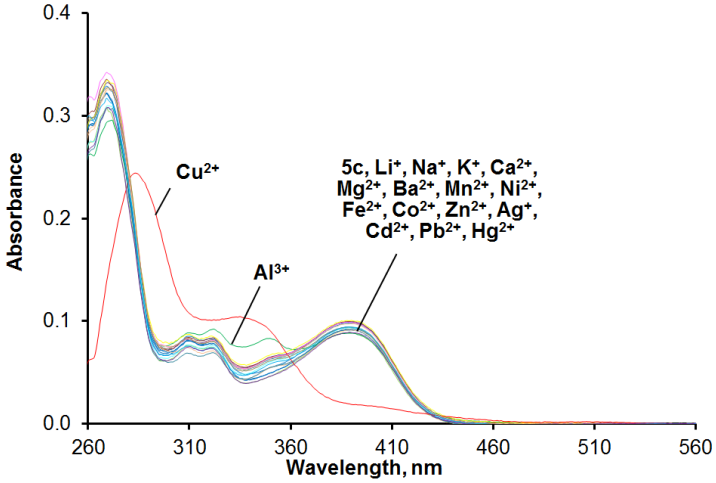


**Figure S14.** UV-vis spectra of **5c** ([**5c**] = 24 μM) in $CH_3CN$ before and after addition of 4 equiv. of metal perchlorates in $CH_3CN$.

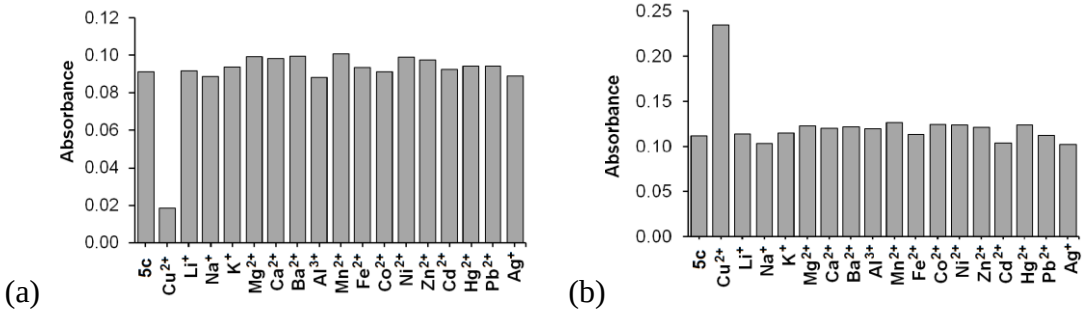


**Figure S15.** Absorbance of **5c** (24 μM solution in $CH_3CN$) in the presence of different metal ions (4 equiv.) at different wavelengths: (a) 390 nm, (b) 288 nm.

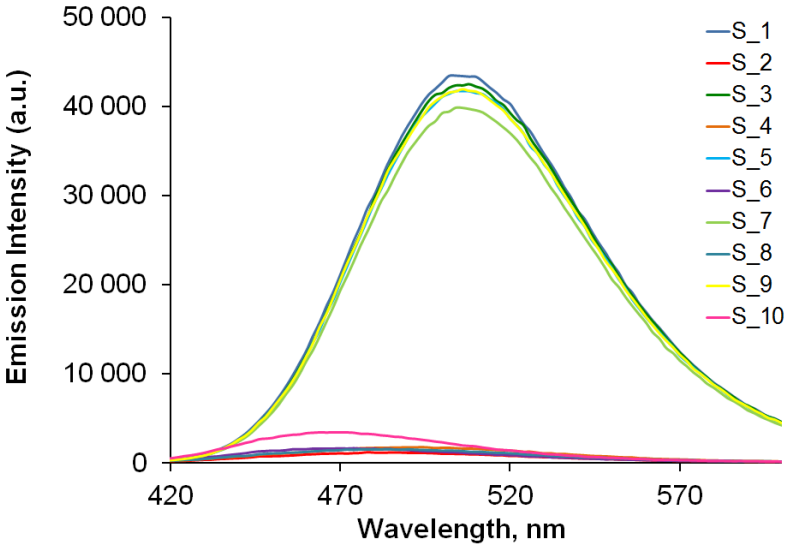


**Figure S16.** Cross-selectivity studies of metal ion binding by ligand **5c** (24 μM solution in $CH_3CN$, $\lambda_{ex}$ = 385 nm) using fluorescrence spectroscopy:

(**S_1**) emission spectrum of **5c**,

(**S_2**) emission spectrum of **5c** after addition of $Cu^{2+}$ (1 equiv.),

(**S_3**) emission spectrum of **5c** after addition of $Li^{+}$, $Na^{+}$, $K^{+}$, $Mg^{2+}$, $Ca^{2+}$, $Ba^{2+}$ (1 equiv. of each metal ion),

(**S_4**) emission spectrum of **5c** after addition of $Li^{+}$, $Na^{+}$, $K^{+}$, $Mg^{2+}$, $Ca^{2+}$, $Ba^{2+}$ (1 equiv. of each metal ion) and $Cu^{2+}$ (1 equiv.)

(**S_5**) emission spectrum of **5c** after addition of $Fe^{2+}$, $Mn^{2+}$, $Co^{2+}$, $Ni^{2+}$, $Zn^{2+}$(1 equiv. of each metal ion),

(**S_6**) emission spectrum of **5c** after addition of $Fe^{2+}$, $Mn^{2+}$, $Co^{2+}$, $Ni^{2+}$, $Zn^{2+}$ (1 equiv. of each metal ion) and $Cu^{2+}$ (1 equiv.)

(**S_7**) emission spectrum of **5c** after addition of $Al^{3+}$ (1 equiv.),

(**S_8**) emission spectrum of **5c** after addition of $Al^{3+}$ (1 equiv) and $Cu^{2+}$ (1 equiv.)

(**S_9**) emission spectrum of **5c** after addition of $Ag^{2+}$, $Hg^{2+}$, $Cd^{2+}$, $Pb^{2+}$ (1 equiv. of each metal ion),

(**S_10**) emission spectrum of **5c** after addition of $Ag^{2+}$, $Hg^{2+}$, $Cd^{2+}$, $Pb^{2+}$ (1 equiv. of each metal ion) and $Cu^{2+}$ (1 equiv.)

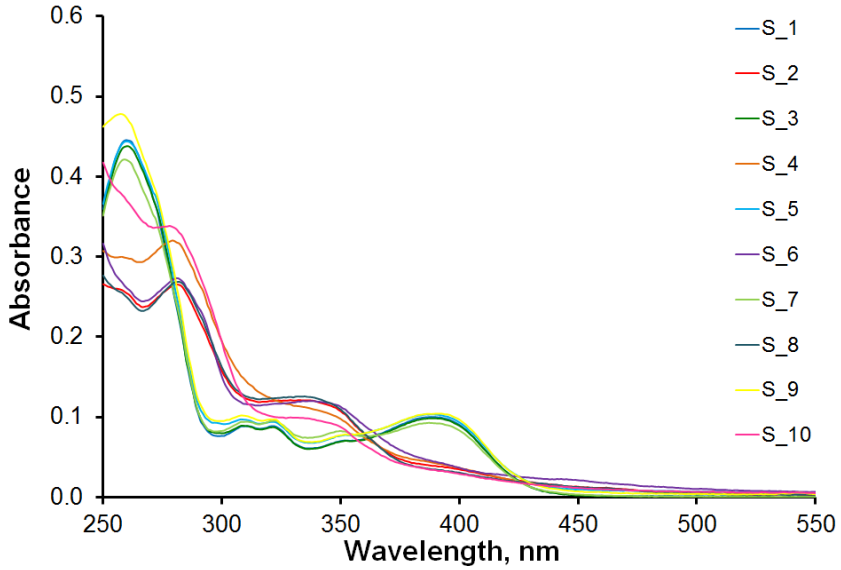


**Figure S17.** Cross-selectivity studies of metal ion binding by ligand **5c** (24 μM solution in $CH_3CN$, $\lambda_{ex}$ = 385 nm) using UV-vis spectroscopy:

(**S_1**) UV-vis spectrum of **5c**,

(**S_2**) UV-vis spectrum of **5c** after addition of $Cu^{2+}$ (1 equiv.),

(**S_3**) UV-vis spectrum of **5c** after addition of $Li^{+}$, $Na^{+}$, $K^{+}$, $Mg^{2+}$, $Ca^{2+}$, $Ba^{2+}$ (1 equiv. of each metal ion),

(**S_4**) UV-vis spectrum of **5c** after addition of $Li^{+}$, $Na^{+}$, $K^{+}$, $Mg^{2+}$, $Ca^{2+}$, $Ba^{2+}$ (1 equiv. of each metal ion) and $Cu^{2+}$ (1 equiv.)

(**S_5**) UV-vis spectrum of **5c** after addition of $Fe^{2+}$, $Mn^{2+}$, $Co^{2+}$, $Ni^{2+}$, $Zn^{2+}$(1 equiv. of each metal ion),

(**S_6**) UV-vis spectrum of **5c** after addition of $Fe^{2+}$, $Mn^{2+}$, $Co^{2+}$, $Ni^{2+}$, $Zn^{2+}$ (1 equiv. of each metal ion) and $Cu^{2+}$ (1 equiv.)

(**S_7**) UV-vis spectrum of **5c** after addition of $Al^{3+}$ (1 equiv.),

(**S_8**) UV-vis spectrum of **5c** after addition of $Al^{3+}$ (1 equiv.) and $Cu^{2+}$ (1 equiv.)

(**S_9**) UV-vis spectrum of **5c** after addition of $Ag^{2+}$, $Hg^{2+}$, $Cd^{2+}$, $Pb^{2+}$ (1 equiv. of each metal ion),

(**S_10**) UV-vis spectrum of **5c** after addition of $Ag^{2+}$, $Hg^{2+}$, $Cd^{2+}$, $Pb^{2+}$ (1 equiv. of each metal ion) and $Cu^{2+}$ (1 equiv.).

3.2 Fluorimetric and spectrophotometric titrations of **5c** with $Cu^{2+}$ ions

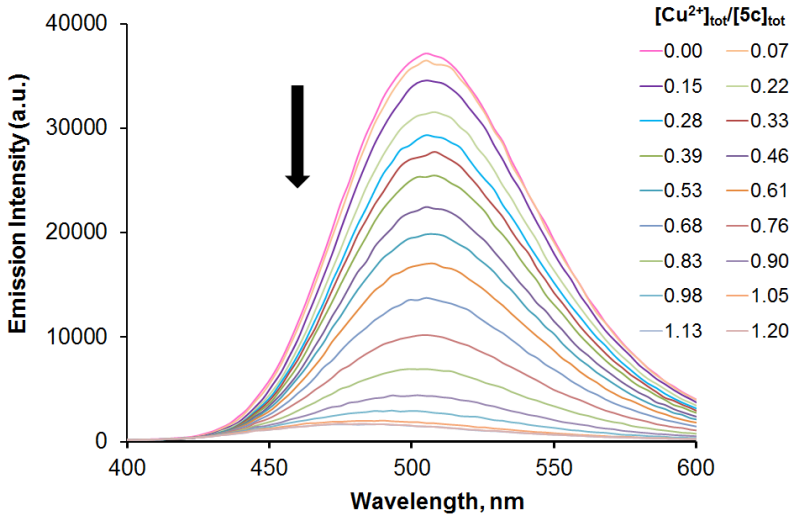


**Figure S18.** Evolution of fluorescence spectrum of **5c** (24 μM solution in $CH_3CN$) upon addition of $Cu(ClO_4)_2$ (0 - 1.2 equiv.) ($\lambda_{ex}$ = 385 nm).

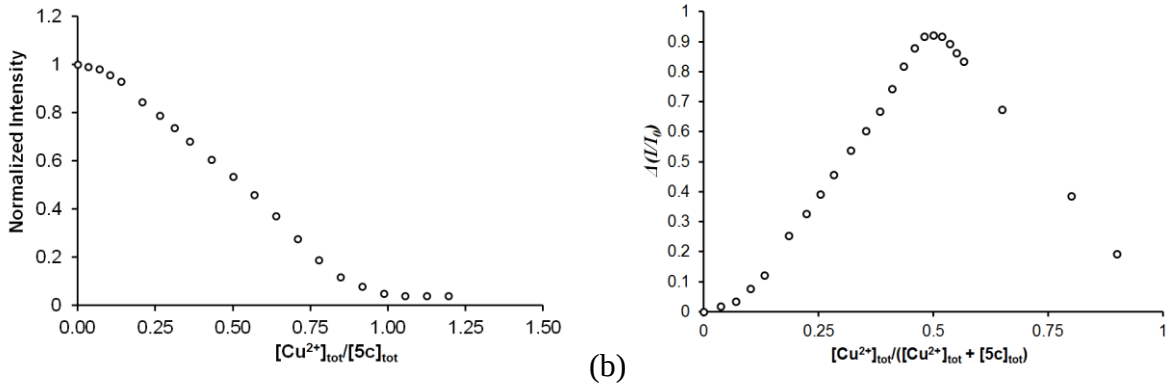


(a) (b)

**Figure S19.** (a) Changes of emission intensities at 505 nm plotted against $[Cu(ClO_4)_2]/[\mathbf{5c}]_{tot}$. (b) Job's plot derived from the titration curve[2].

Stability constants calculated using SPECFIT[1]

$lg(\beta_{Cu(\mathbf{5c})2})$ = 14.5±0.3 , $lg(\beta_{Cu(\mathbf{5c})})$ = 8.0±0.2

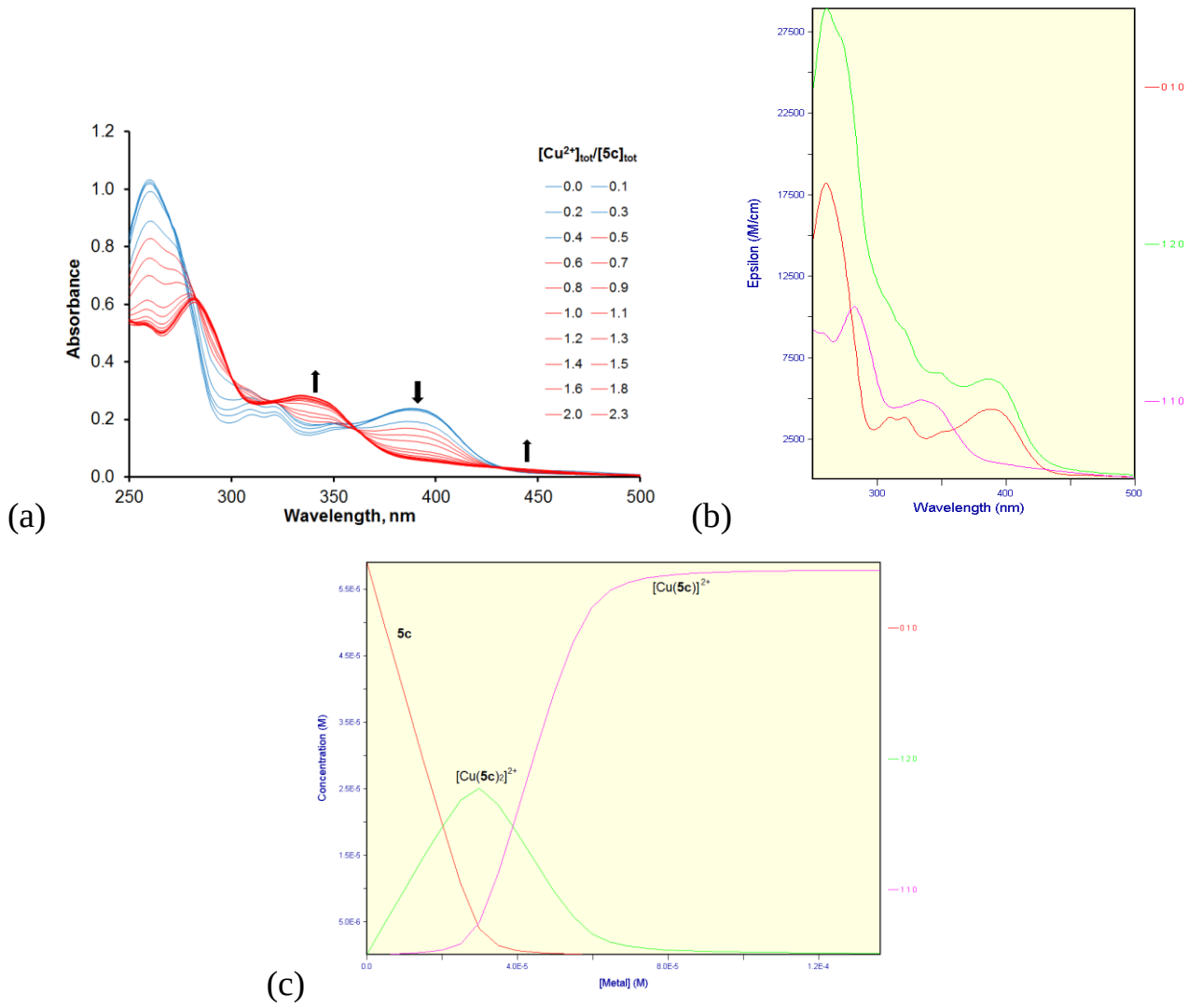


**Figure S20.** (a) Evolution of UV–vis spectrum of **5c** (60 μM solution in $CH_3CN$) upon addition of $Cu(ClO_4)_2$ (0 - 2.3 equiv.). (b) UV-vis spectra of **5c** (red), $[Cu(\mathbf{5c})_2]^{2+}$ (green) and $[Cu(\mathbf{5c})]^{2+}$ (magenta) calculated using SPECFIT[1]. (c) Species distribution diagram for the $Cu^{2+}$/**5c** system in $CH_3CN$ calculated using SPECFIT[1].

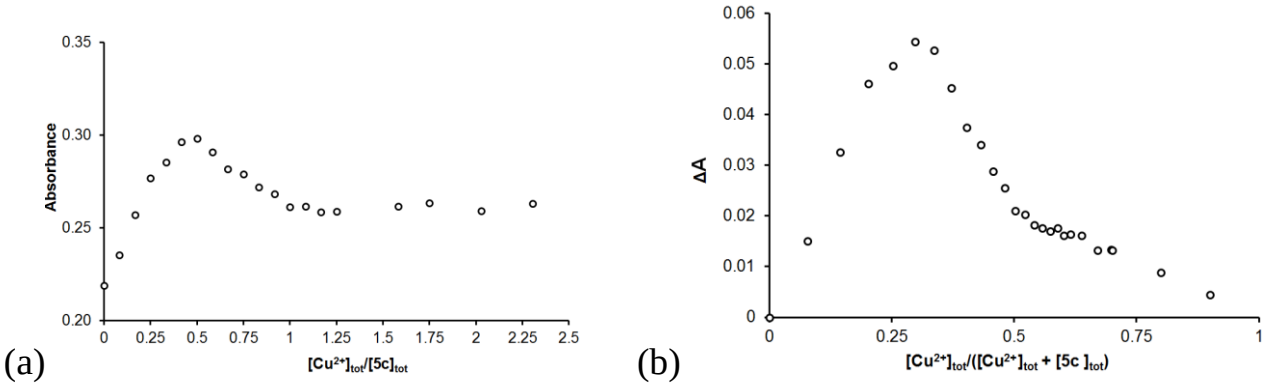


**Figure S21.** (a) Changes of absorbance at 311 nm plotted against $[Cu(ClO_4)_2]/[\mathbf{5c}]_{tot}$. (b) Job's plot derived from the titration curve[2].

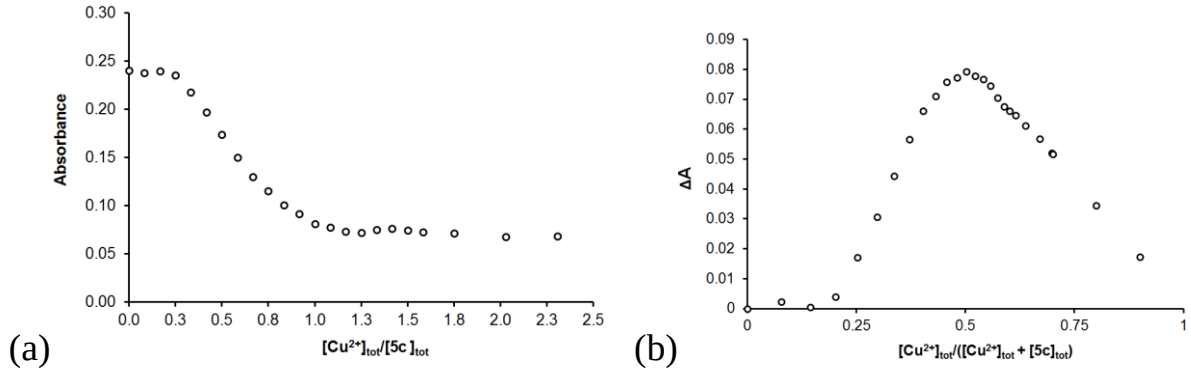


**Figure S22.** (a) Changes of absorbance at 385 nm plotted against $[Cu(ClO_4)_2]/[\mathbf{5c}]_{tot}$. (b) Job's plot derived from the titration curve[2].

Stability constants calculated using SPECFIT[1]

$\lg(\beta_{Cu(\mathbf{5c})2}) = 14.5\pm0.2$ , $\lg(\beta_{Cu(\mathbf{5c})}) = 8.4\pm0.2$

## 4. Studies of binding metal ions by 10

4.1. Fluorimetric and UV-vis studies of binding metal ions by **10**

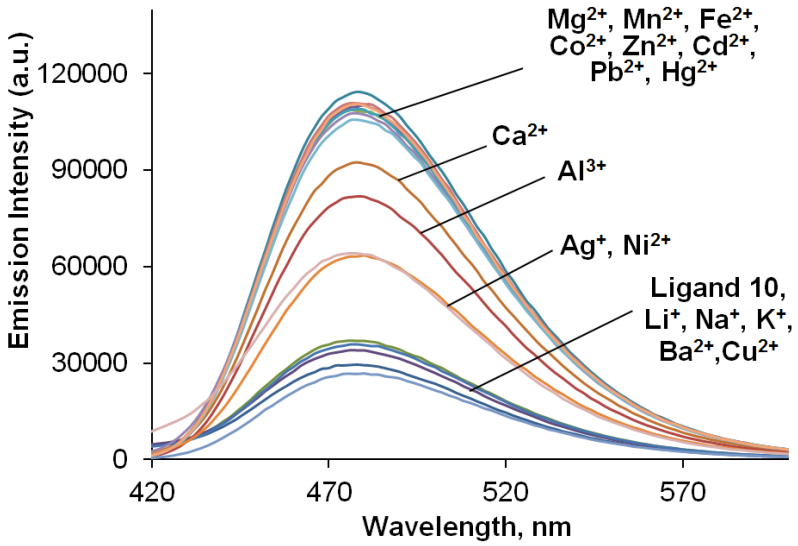


**Figure S23.** Fluorescence spectra of **10** ([**10**] = 20 μM) in $CH_3CN$ before and after addition of 4 equiv. of metal perchlorates in $CH_3CN$ ($\lambda_{ex}$ = 390 nm).

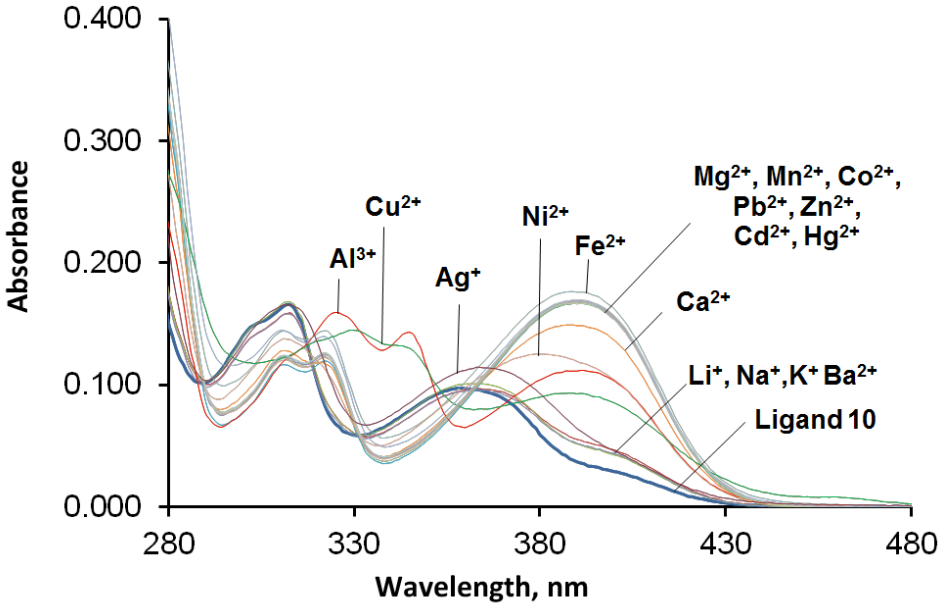


**Figure S24.** UV-vis spectra of **10** ([**10**] = 20 μM) in $CH_3CN$ before and after addition of 4 equiv. of metal perchlorates in $CH_3CN$.

4.2 Fluorimetric and spectrophotometric titrations of **10** with $Cu^{2+}$ ions

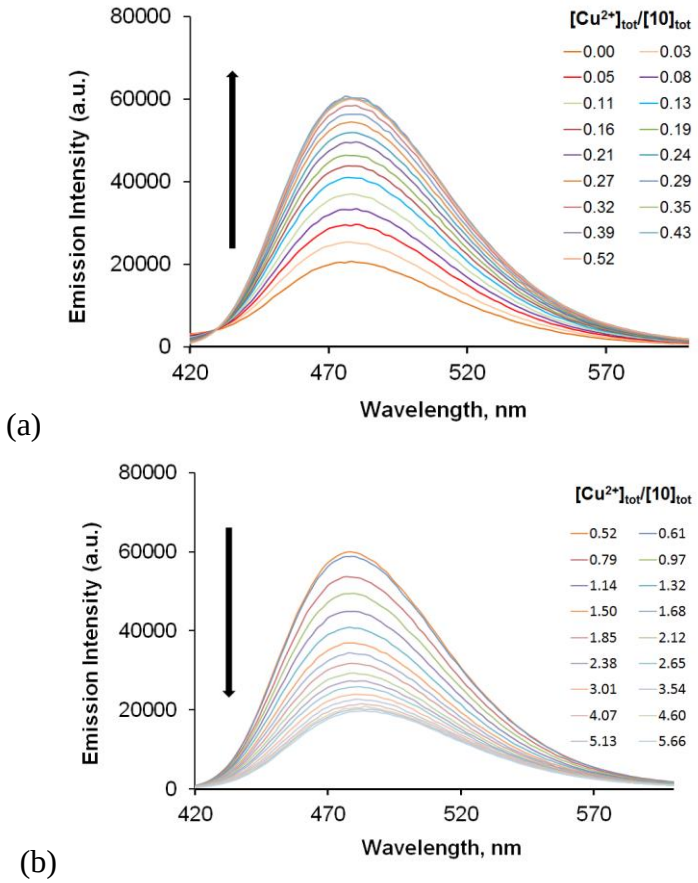


**Figure S25.** (a) Evolution of fluorescence spectrum of **10** (9 μM solution in $CH_3CN$) upon addition of $Cu(ClO_4)_2$ (0 - 0.5 equiv.) ($\lambda_{ex}$ = 390 nm). (b) Evolution of luminescence spectrum of **10** (9 μM solution in $CH_3CN$) upon addition of $Cu(ClO_4)_2$ (0.5 - 5.7 equiv.) ($\lambda_{ex}$ = 390 nm).

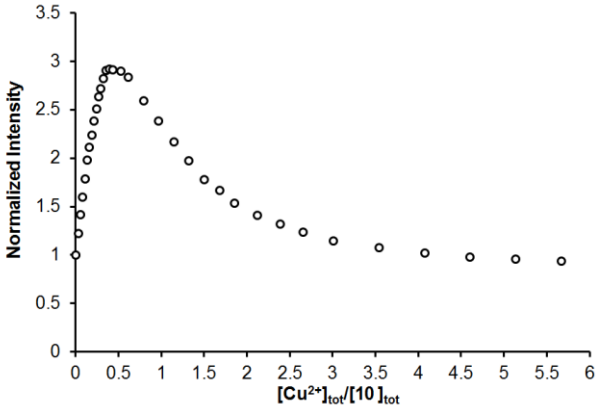


**Figure S26.** Changes of emission intensities at 478 nm plotted against $[Cu(ClO_4)_2]/[\mathbf{10}]_{tot}$.
Stability constants calculated using SPECFIT[1]
$lg(\beta_{Cu(\mathbf{10})2})$ = 11.3±0.2 , $lg(\beta_{Cu(\mathbf{10})})$ = 6.1±0.1

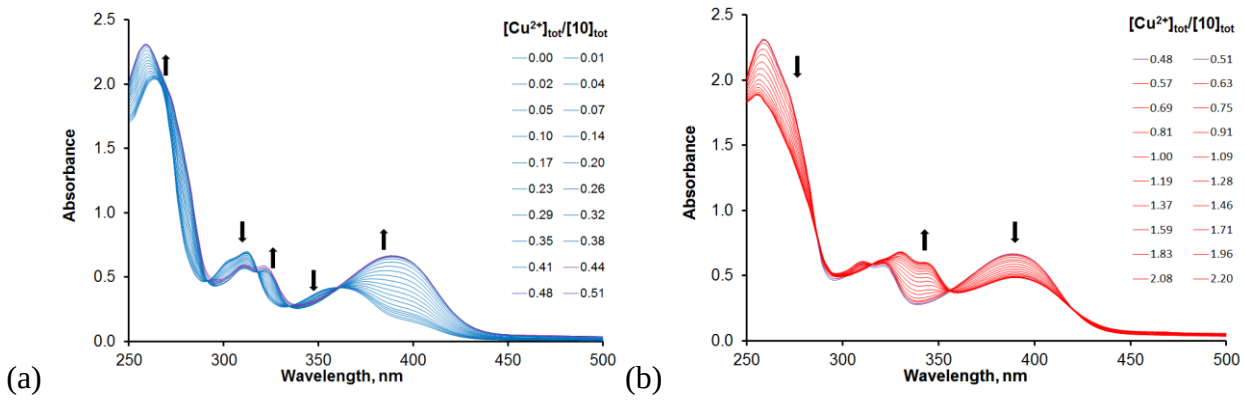


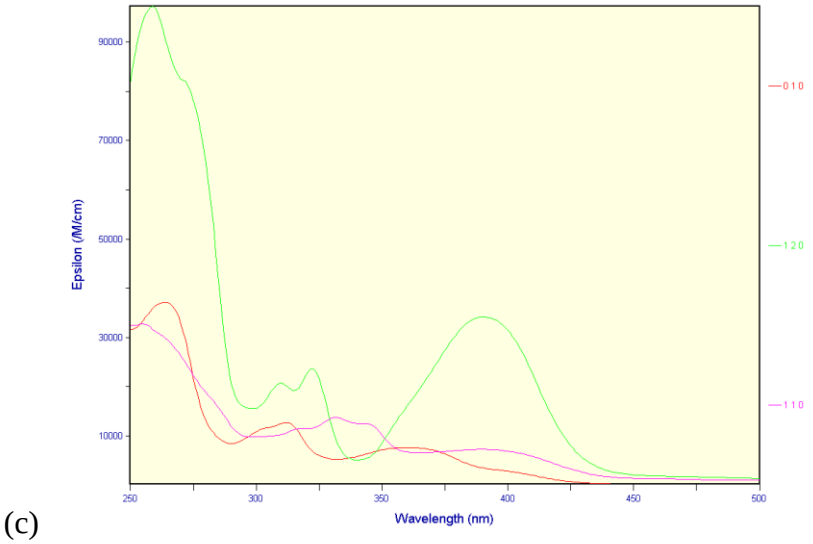


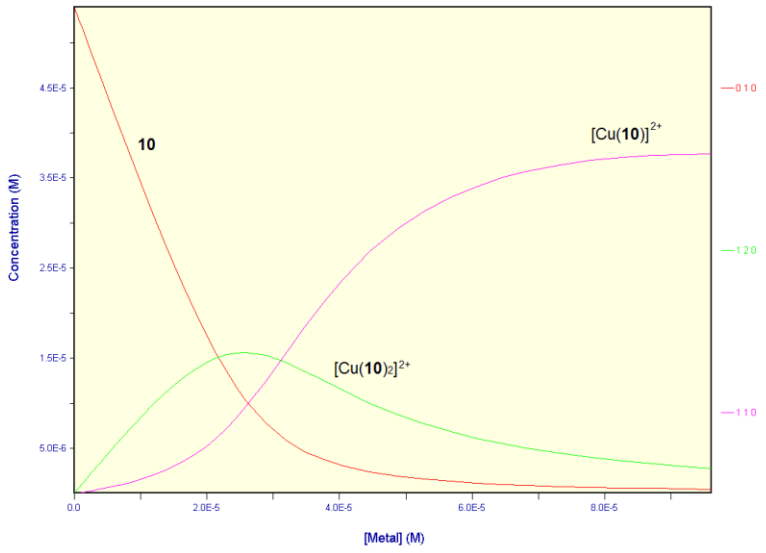


**Figure S27.** Evolution of UV–vis spectrum of **10** (54 μM solution in $CH_3CN$) upon addition of $Cu(ClO_4)_2$ (0 - 0.5 equiv.). (b) Evolution of UV–vis spectrum of **10** (54 μM solution in $CH_3CN$) upon addition of $Cu(ClO_4)_2$ (0.5 - 2.2 equiv.). (c) UV-vis spectra of **10** (red), $[Cu(\mathbf{10})_2]^{2+}$ (green) and $[Cu(\mathbf{10})]^{2+}$ (magenta) calculated using SPECFIT[1]. (d) Species distribution diagram for the $Cu^{2+}$/**10** system in $CH_3CN$ calculated using SPECFIT[1].

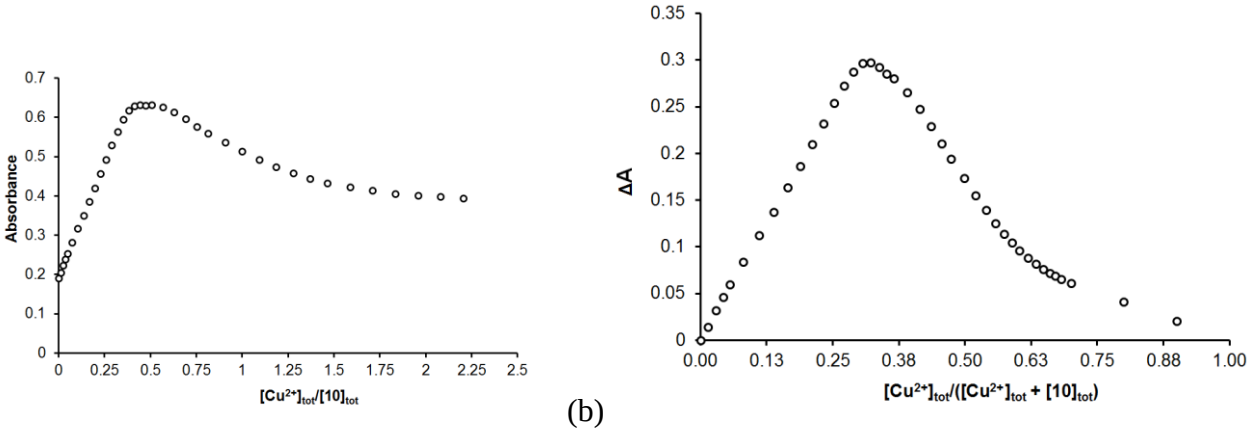


(a) (b)

**Figure S28.** (a) Changes of absorbance at 390 nm plotted against $[Cu(ClO_4)_2]/[\mathbf{10}]_{tot}$. (b) Job's plot derived from the titration curve[2].

Stability constants calculated using SPECFIT[1]

$\lg(\beta_{Cu(\mathbf{10})2}) = 11.7\pm0.2$ , $\lg(\beta_{Cu(\mathbf{10})}) = 6.4\pm0.1$

4.3 Fluorimetric and spectrophotometric titrations of **10** with $Zn^{2+}$ ions

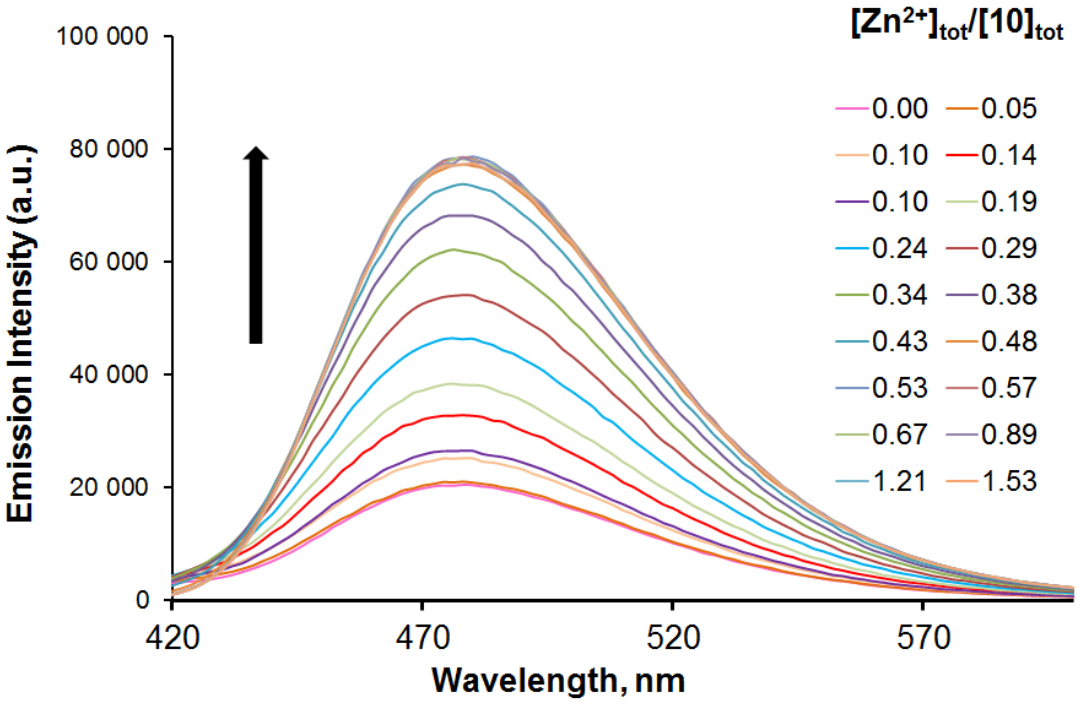


**Figure S29.** Evolution of fluoresence spectrum of **10** (9 μM solution in $CH_3CN$) upon addition of $Zn(ClO_4)_2$ (0 - 1.5 equiv.) ($\lambda_{ex}$ = 390 nm).

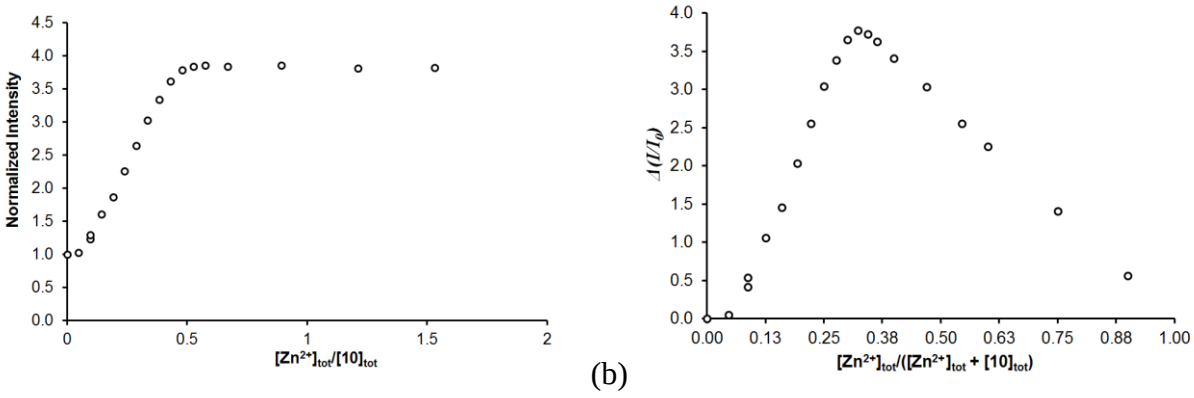


(a) (b)

**Figure S30.** (a) Changes of emission intensities at 478 nm plotted against $[Zn(ClO_4)_2]/[\mathbf{10}]_{tot}$. (b) Job's plot derived from the titration curve[2].

Stability constants calculated using SPECFIT[1]

$lg(\beta_{Zn(\mathbf{10})4})$ = [19.9] , $lg(\beta_{Zn(\mathbf{10})2})$ = 10.7±0.4

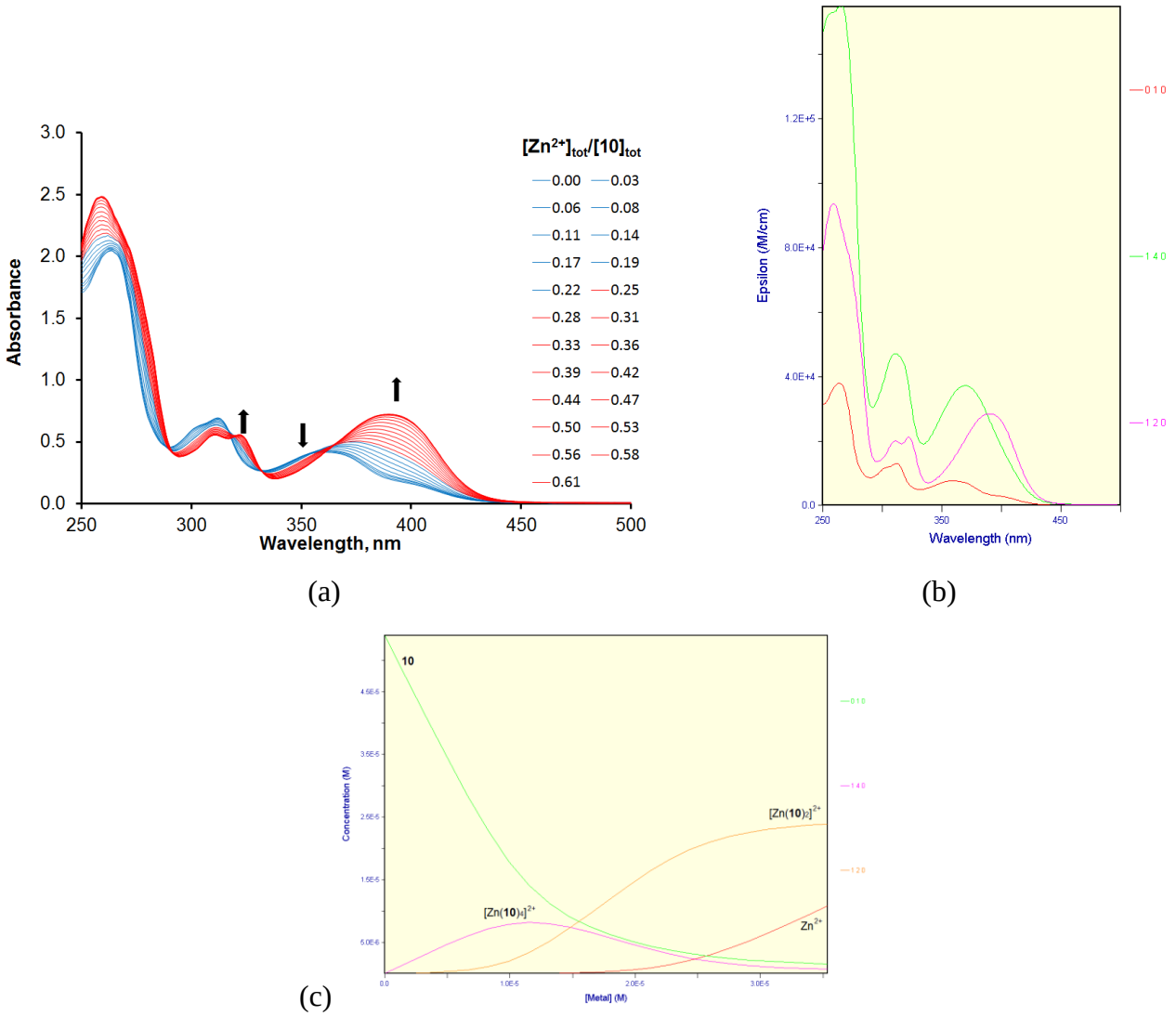


(a) (b)

(c)

**Figure S31.** (a) Evolution of UV–vis spectrum of **10** (54 μM solution in $CH_3CN$) upon addition of $Zn(ClO_4)_2$ (0 - 0.6 equiv.). (b) UV-vis spectra of **10** (red), $[Zn(\mathbf{10})_4]^{2+}$ (green) and $[Zn(\mathbf{10})_2]^{2+}$ (magenta) calculated using SPECFIT[1]. (c) Species distribution diagram for the $Zn^{2+}$/**10** system in $CH_3CN$ calculated using SPECFIT[1].

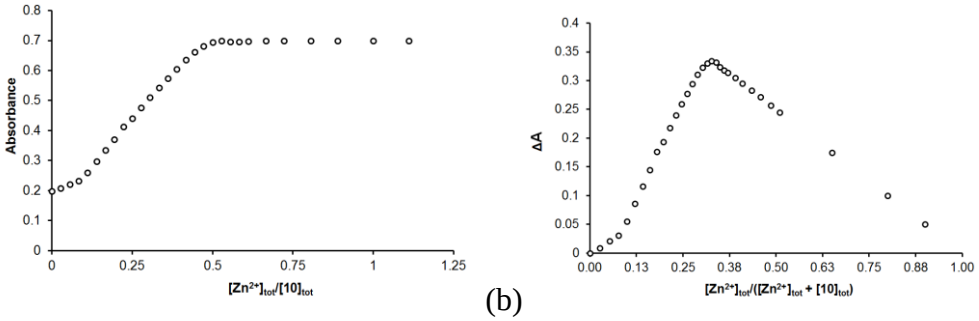


(a) (b)

**Figure S32.** (a) Changes of absorbance at 390 nm plotted against $[Zn(ClO_4)_2]/[\mathbf{10}]_{tot}$. (b) Job's plot derived from the titration curve[2].

Stability constants calculated using SPECFIT[1]

$\lg(\beta_{Zn(\mathbf{10})4}) = 20.0 \pm 0.4$ , $\lg(\beta_{Zn(\mathbf{10})2}) = 11.9 \pm 0.2$

4.4 NMR titrations of **10** with $Zn^{2+}$ ions

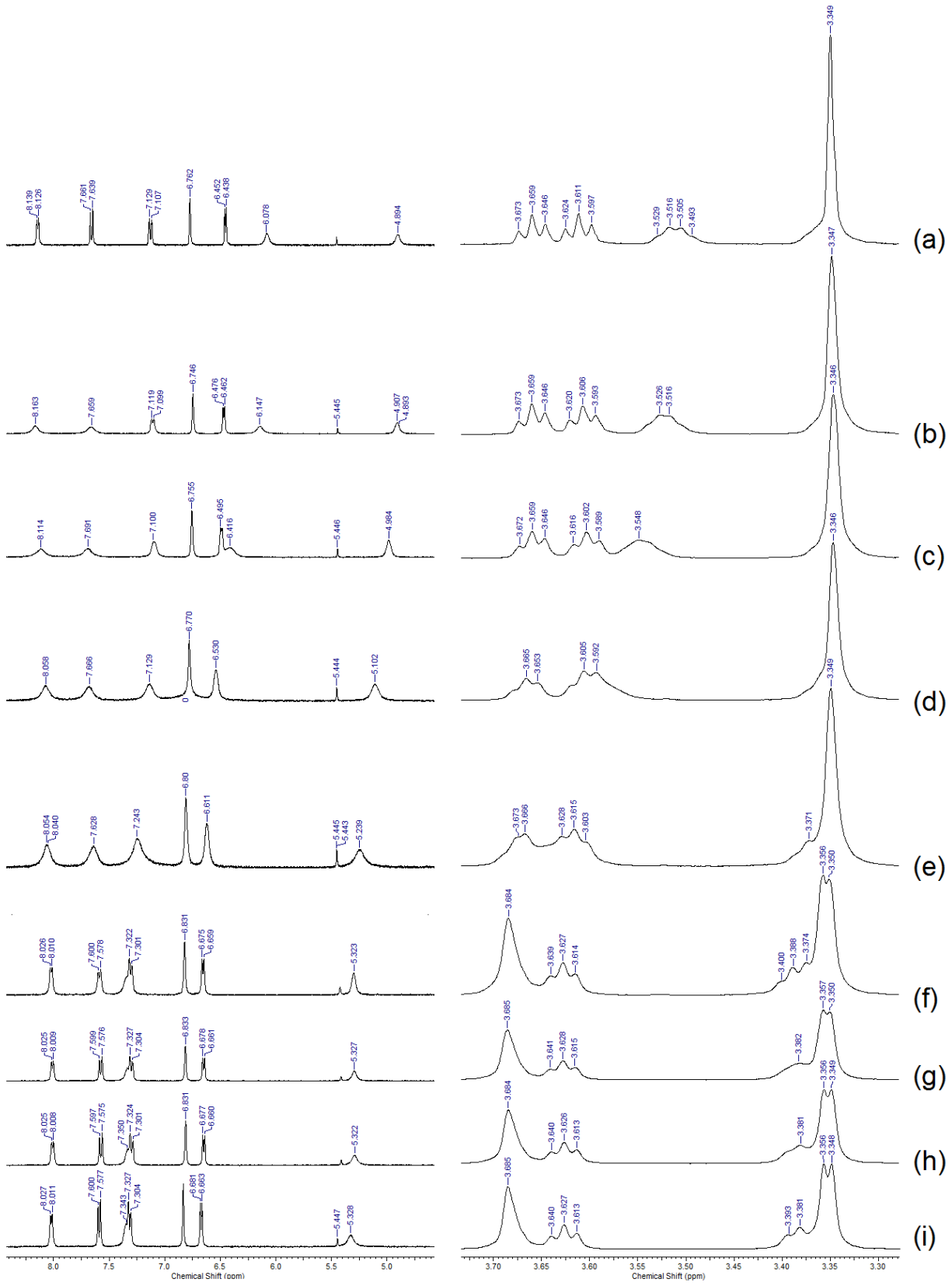


**Figure S33.** 400 MHz H NMR spectra of 10 in $CD_3CN$ at 298 K before (a) and after addition of 0.1 (b), 0.2 (c), 0.3 (d), 0.4 (e), 0.5 (f), 0.6 (g), 0.7 (h) and 0.8 (i) equiv. of zinc perchlorate.

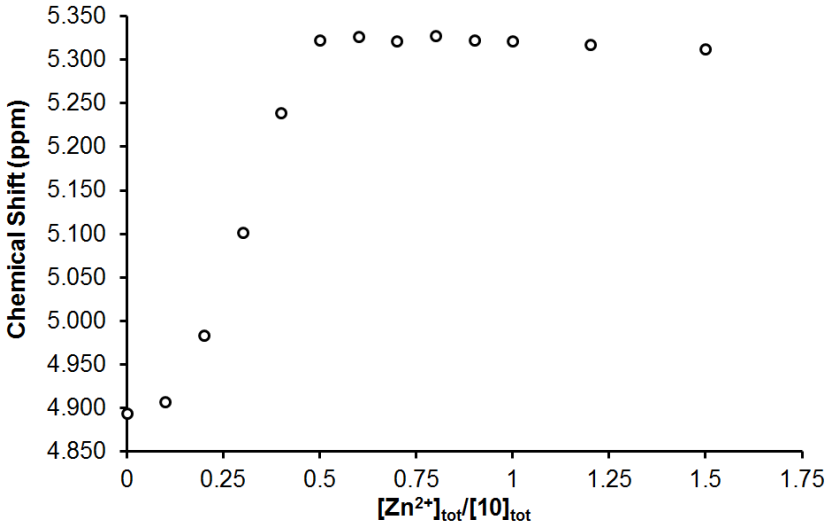


**Figure S34.** Changes of the chemical shift of N<u>H</u>-proton plotted against $[Zn(ClO_4)_2]/[\mathbf{10}]_{tot}$.

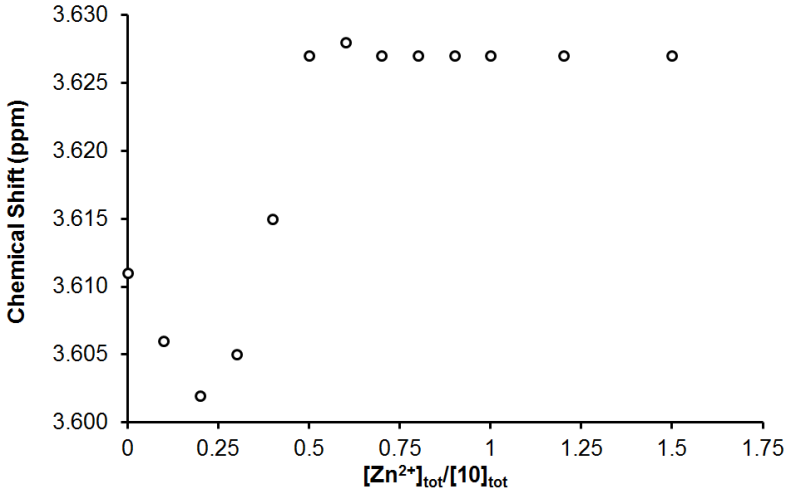


**Figure S35.** Changes of the chemical shift of C<u>H</u>$_2$O-proton plotted against $[Zn(ClO_4)_2]/[\mathbf{10}]_{tot}$.

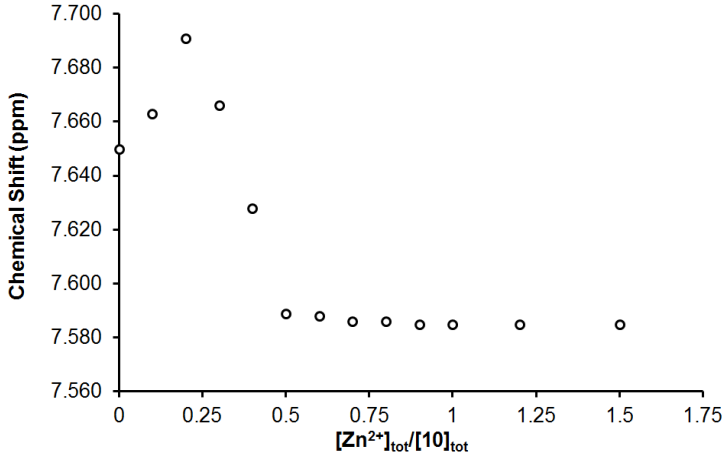


**Figure S36.** Changes of the chemical shift of $H^8$(Quin)-proton plotted against $[Zn(ClO_4)_2]/[\mathbf{10}]_{tot}$.

## 5. Supposed mechanism of quenching fluorescence of ligands 10 and 5c

Supposed mechanism of quenching luminescence of ligand **10** by $Cu^{2+}$ ions

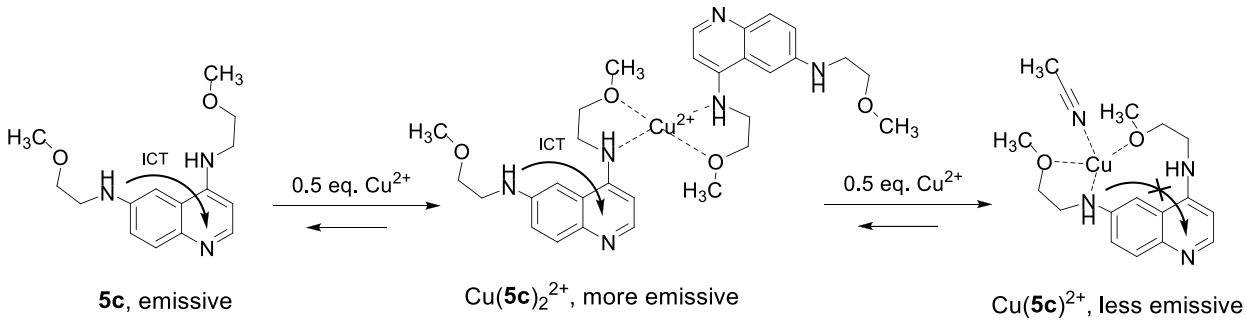


**5c**, emissive — $Cu(\mathbf{5c})_2^{2+}$, more emissive — $Cu(\mathbf{5c})^{2+}$, less emissive

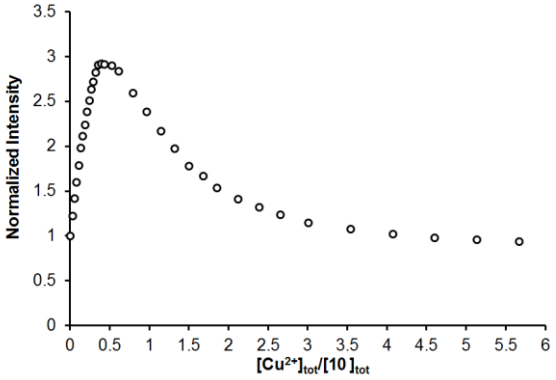


Supposed mechanism of quenching luminescence of ligand **5c** by $Cu^{2+}$ ions

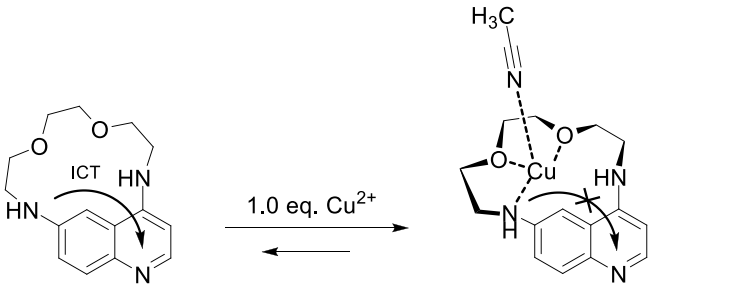


**5c**, emissive — $Cu(\mathbf{5c})^{2+}$, non-emissive

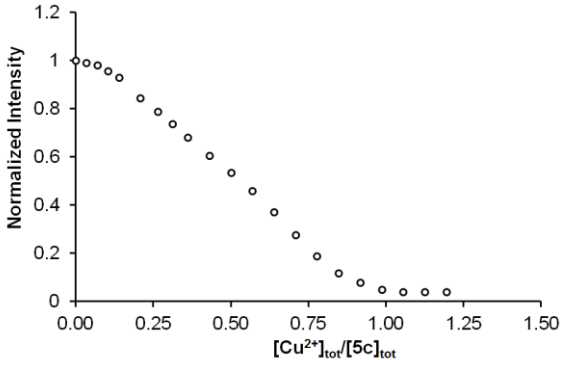

## 6. NMR spectra

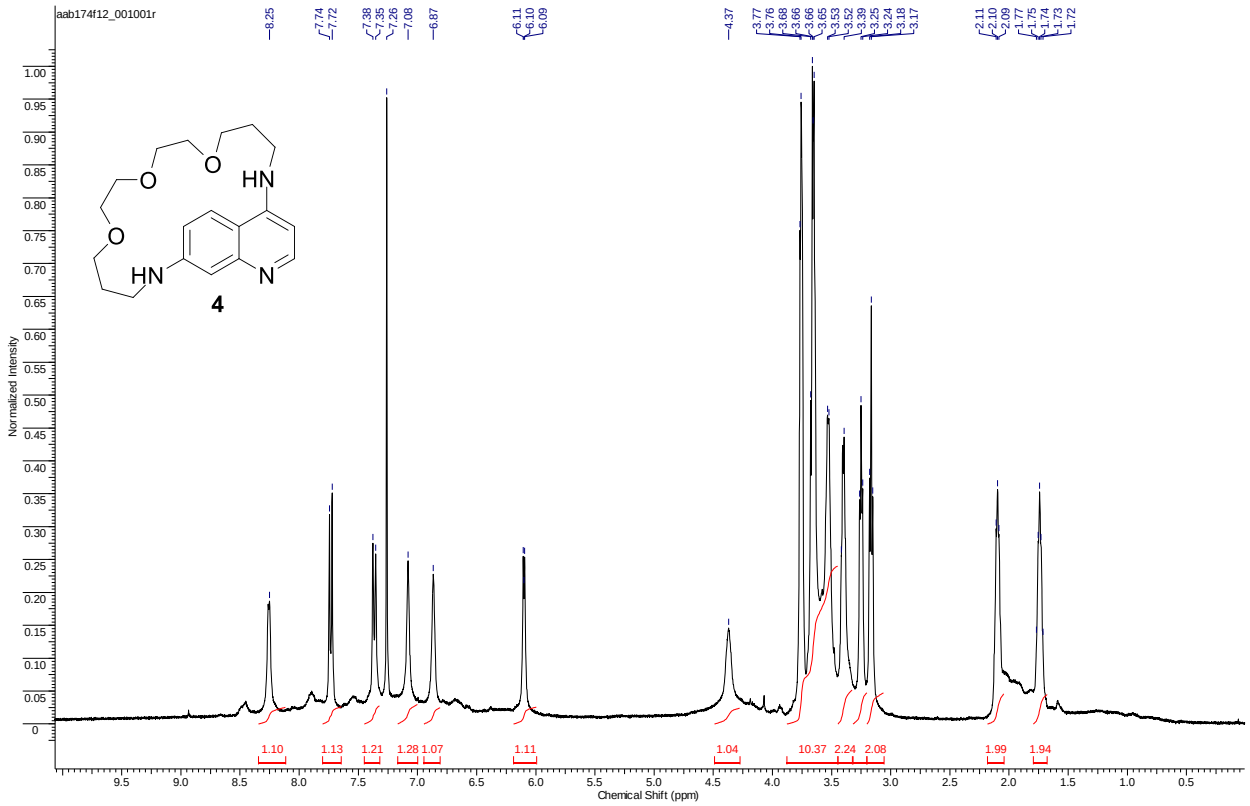


**Figure S37.** $^{1}$H NMR spectrum of **4** ($CDCl_3$, 400MHz, 300K).

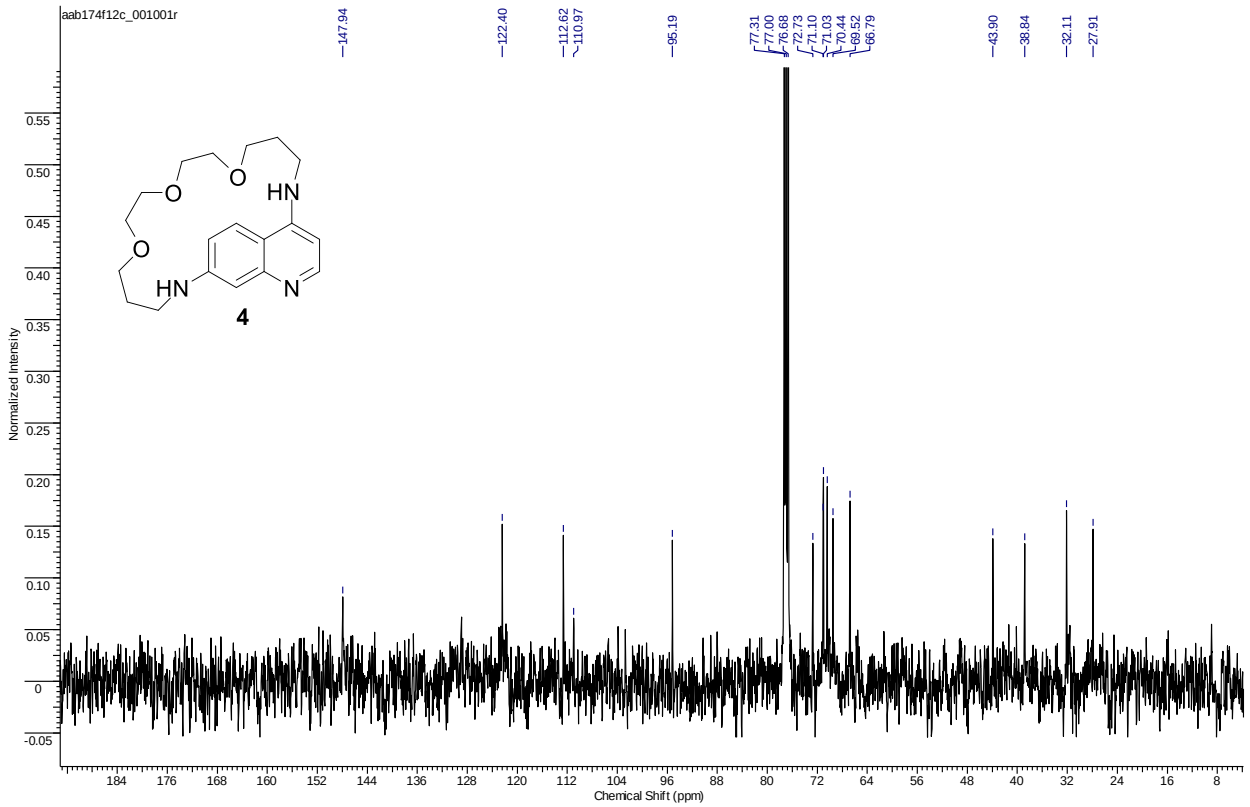


**Figure S38.** $^{13}$C NMR spectrum of **4** ($CDCl_3$, 400MHz, 300K). (4 quaternary carbon atoms were not unambiguously assigned because of broadening of the signals and low concentration)

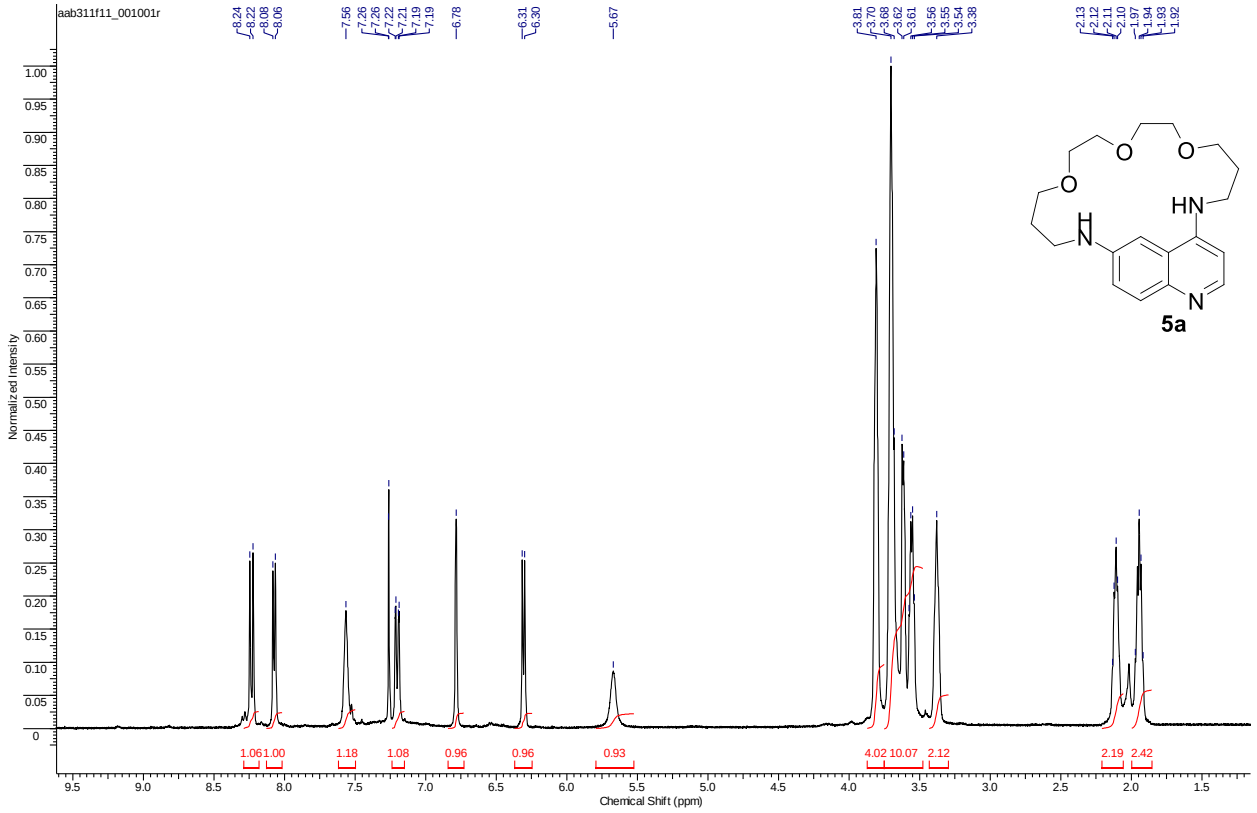


**Figure S39.** $^{1}$H NMR spectrum of **5a** ($CDCl_3$, 400MHz, 300K).

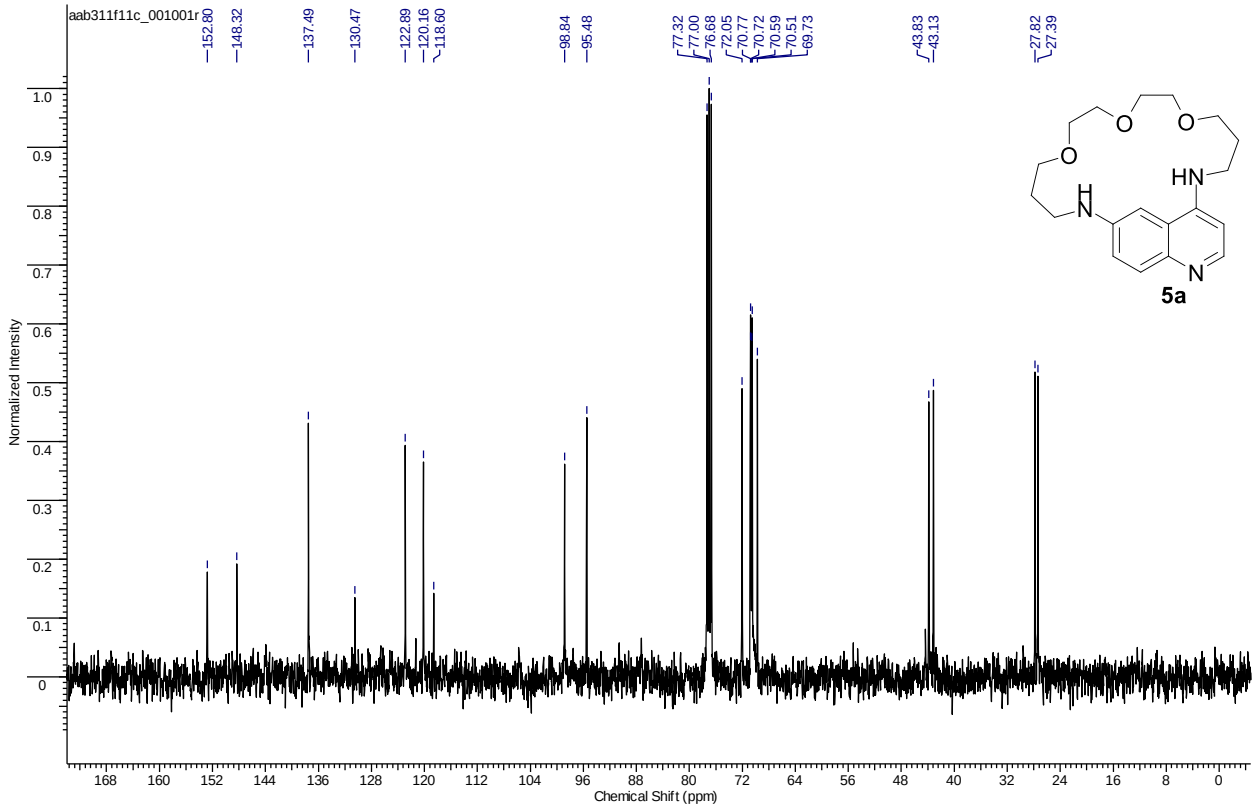


**Figure S40.** $^{13}$C NMR spectrum of **5a** ($CDCl_3$, 400MHz, 300K).

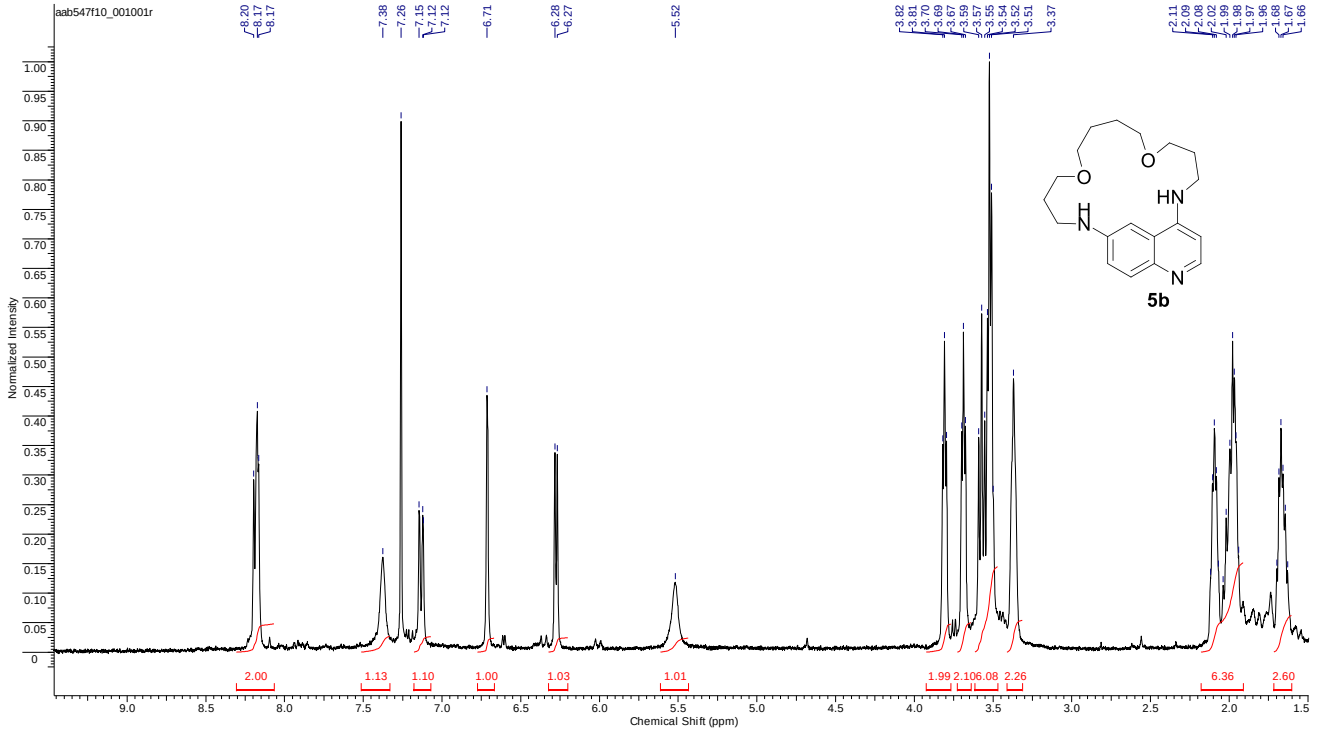


**Figure S41.** $^{1}$H NMR spectrum of **5b** ($CDCl_3$, 400MHz, 300K).

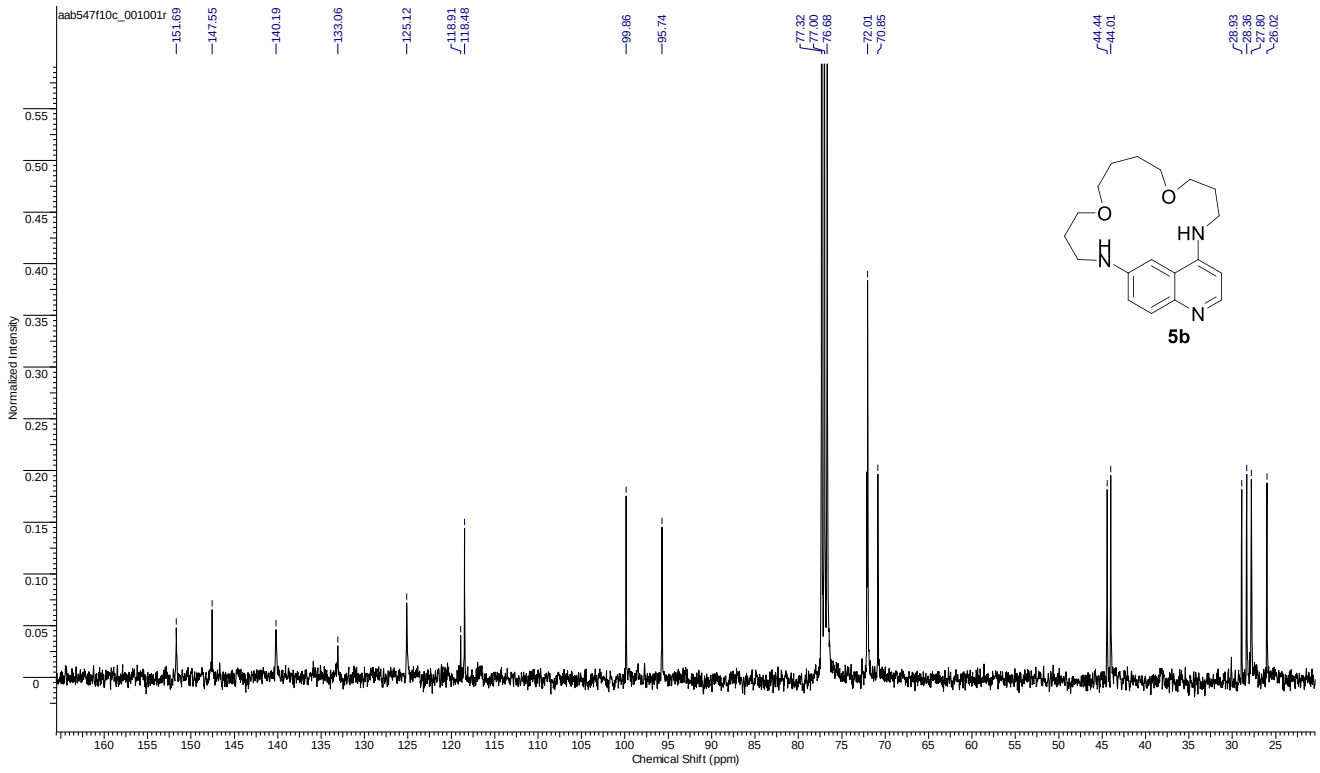


**Figure S42.** $^{13}$C NMR spectrum of **5b** ($CDCl_3$, 400MHz, 300K).

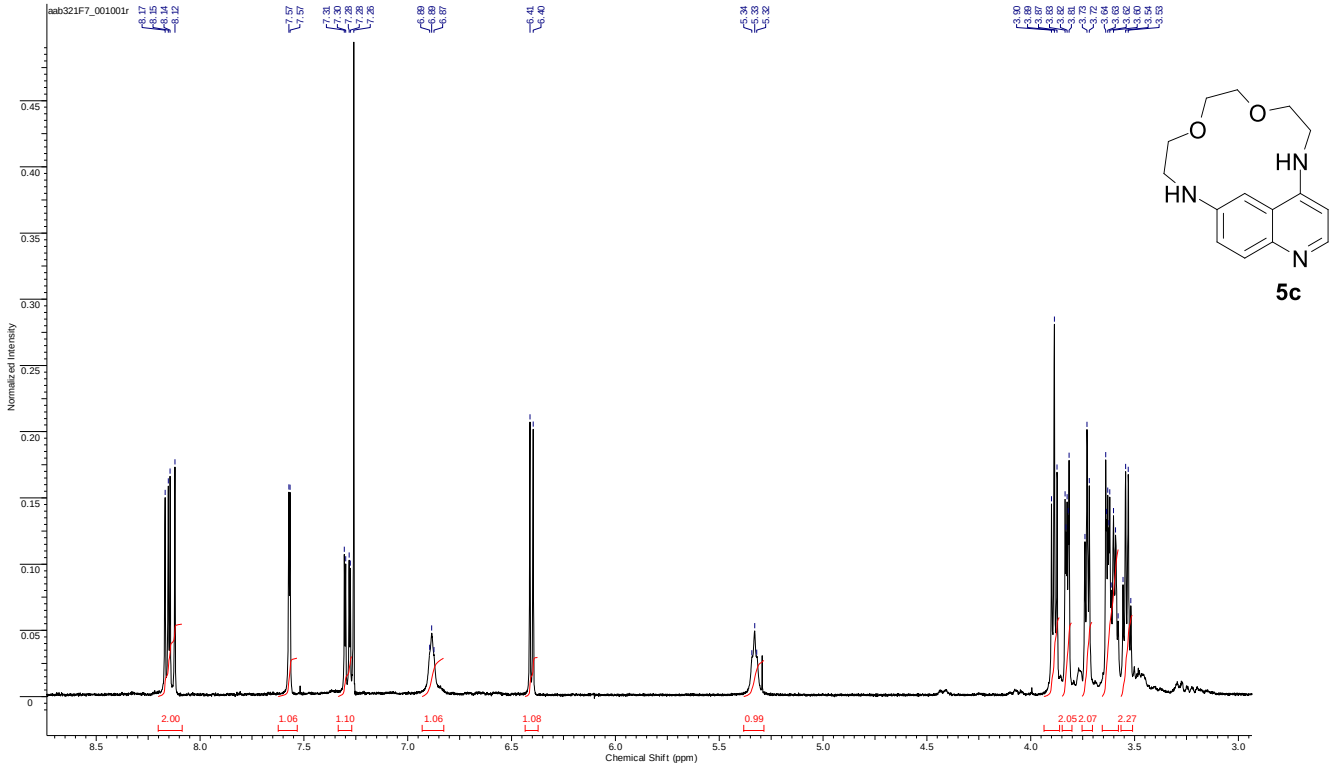


**Figure S43.** $^{1}$H NMR spectrum of **5c** ($CDCl_3$, 400MHz, 300K).

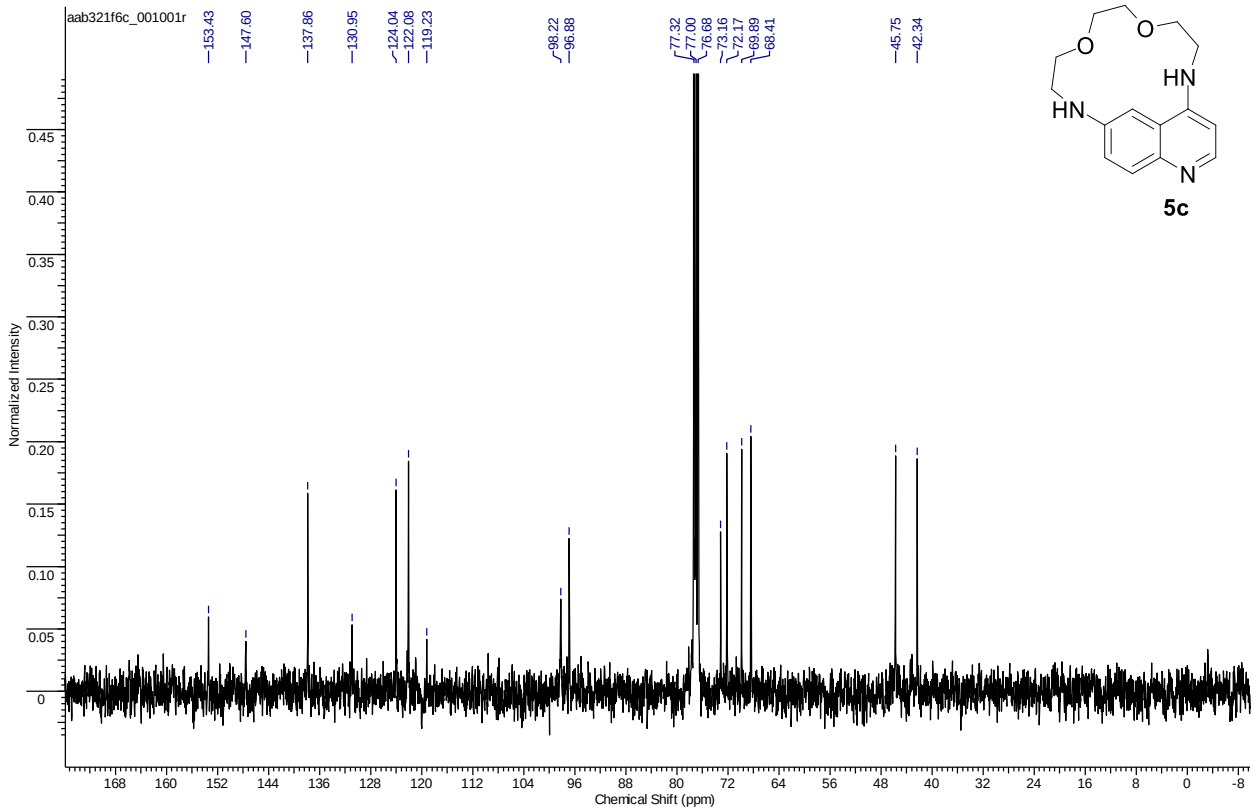


**Figure S44.** $^{13}$C NMR spectrum of **5c** ($CDCl_3$, 400MHz, 300K).

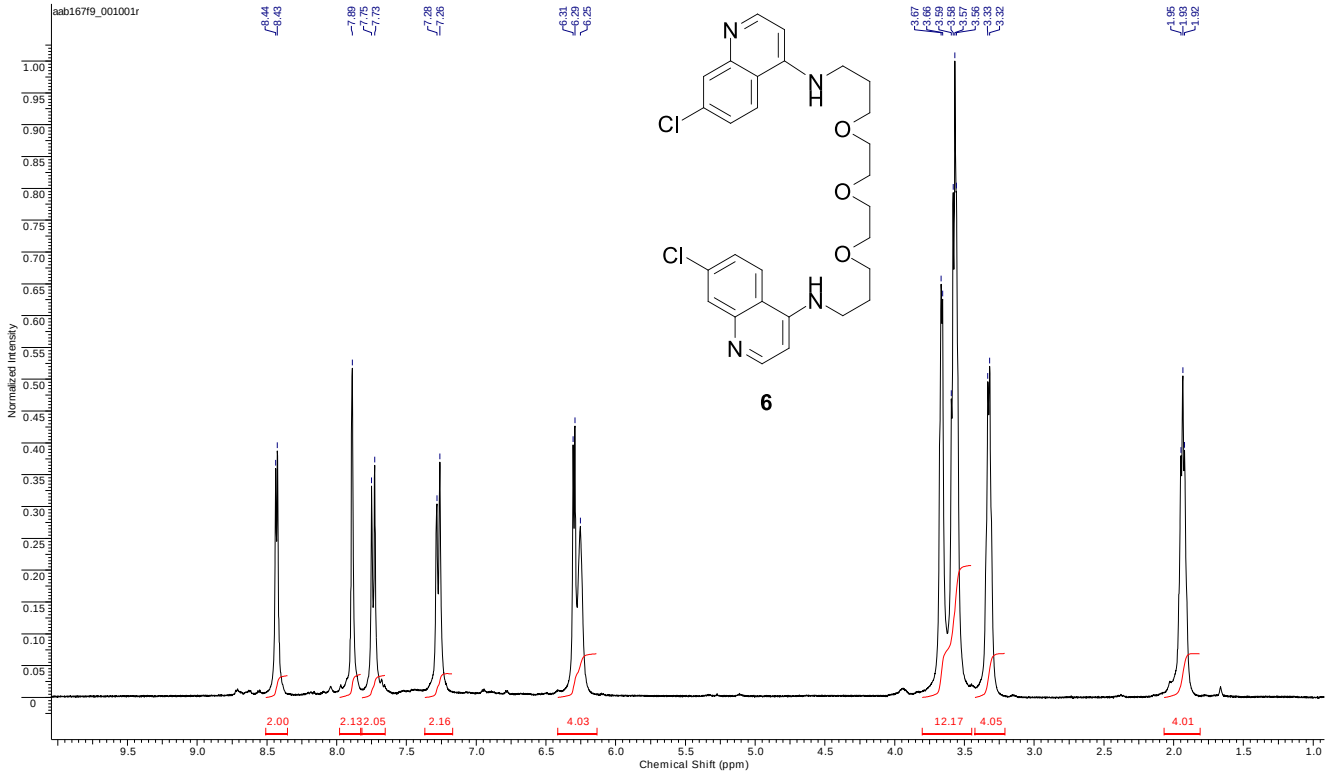


**Figure S45.** $^{1}$H NMR spectrum of **6** ($CDCl_3$, 400MHz, 300K).

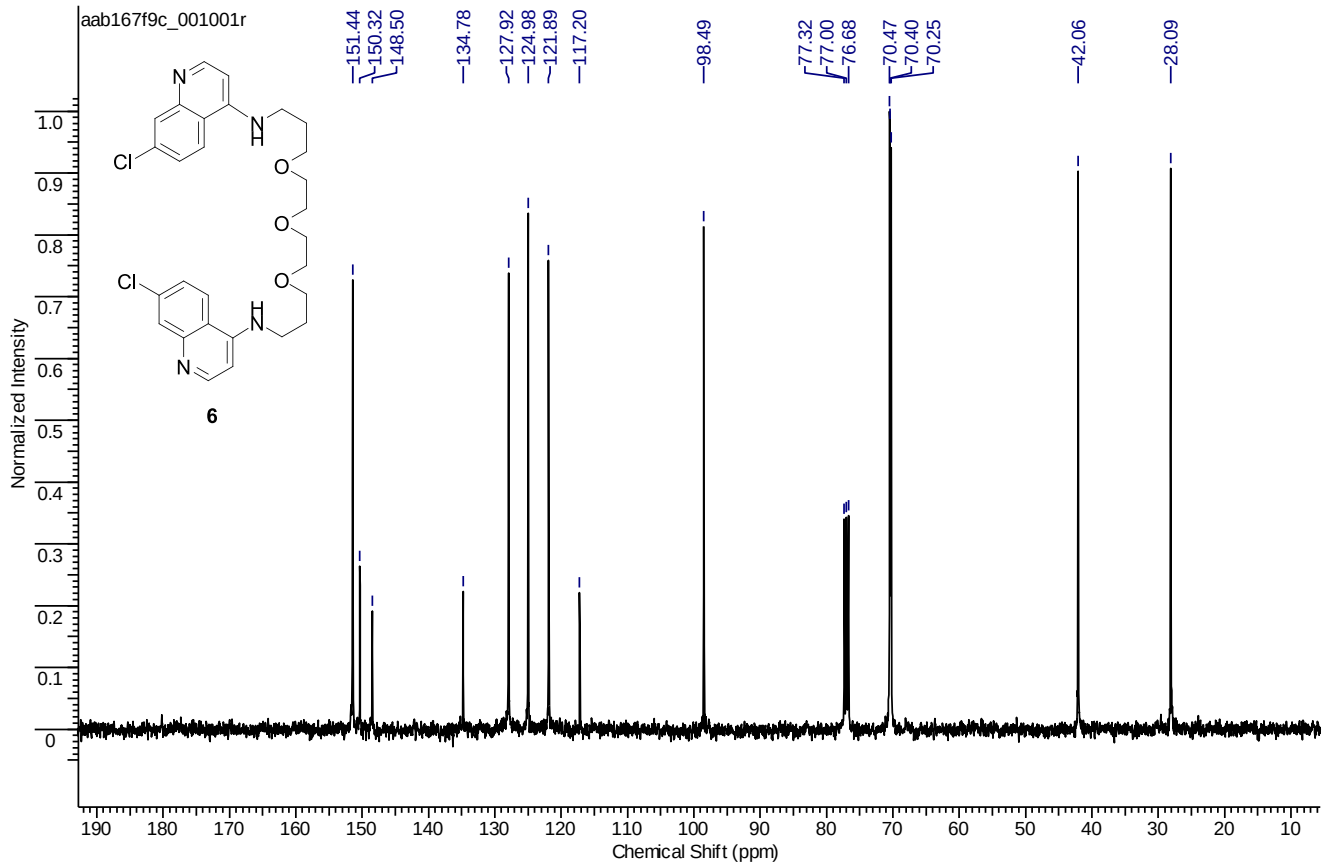


**Figure S46.** $^{13}$C NMR spectrum of **6** ($CDCl_3$, 400MHz, 300K).

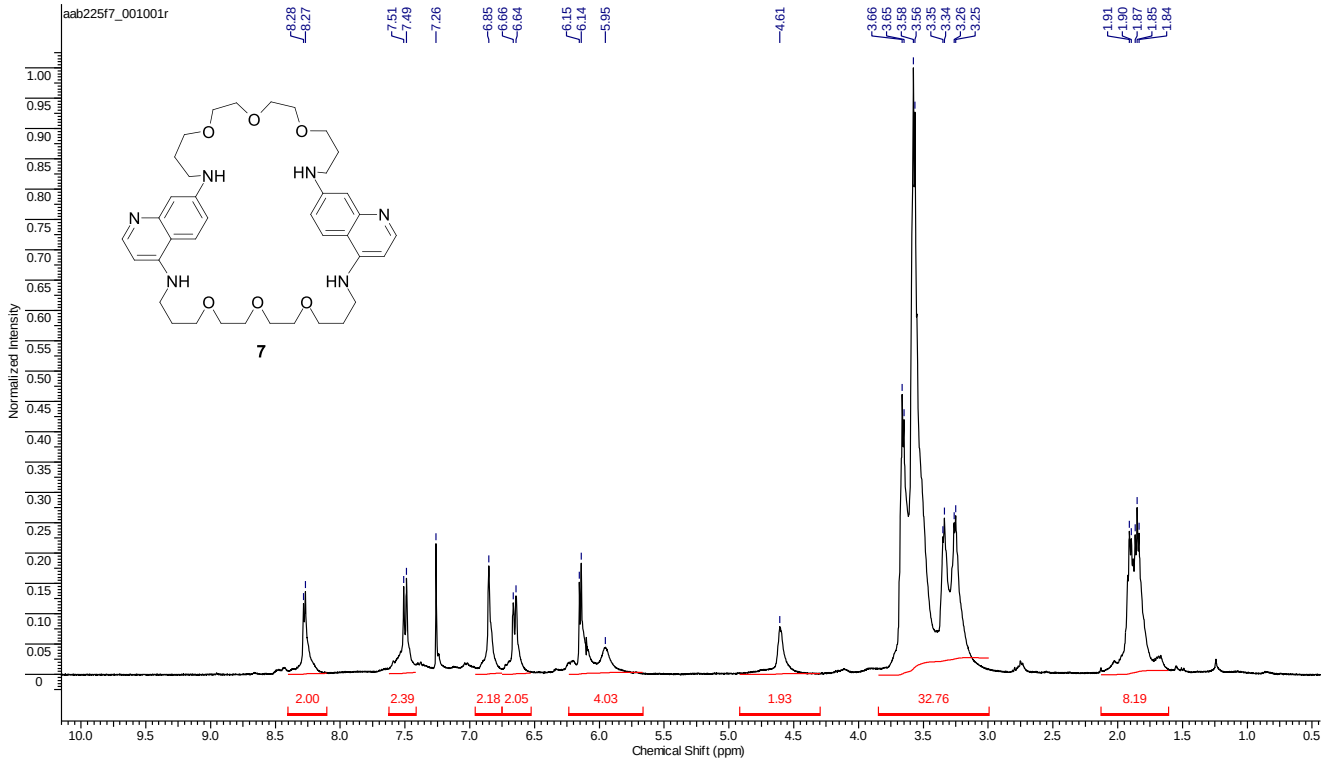


**Figure S47.** $^{1}$H NMR spectrum of **7** ($CDCl_3$, 400MHz, 300K).

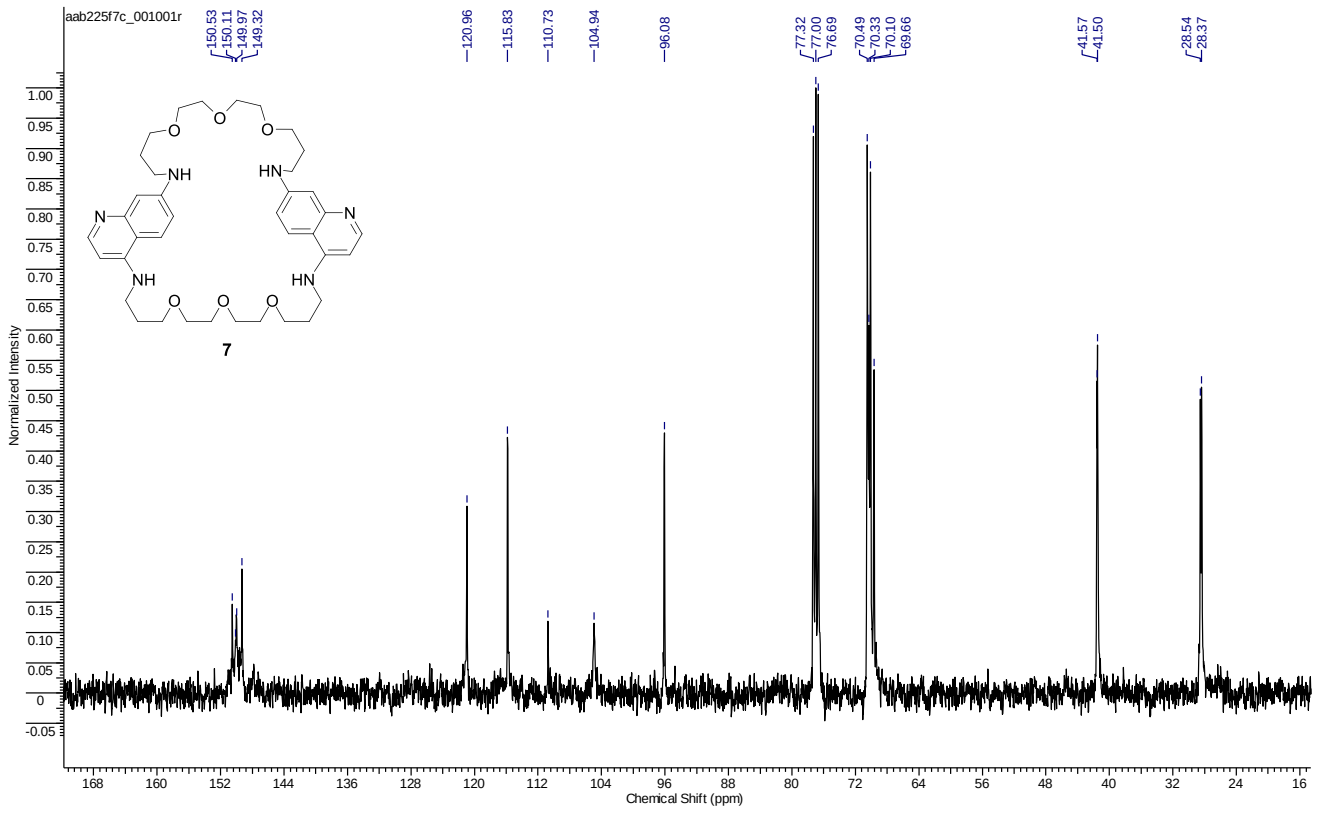


**Figure S48.** $^{13}$C NMR spectrum of **7** ($CDCl_3$, 400MHz, 300K).

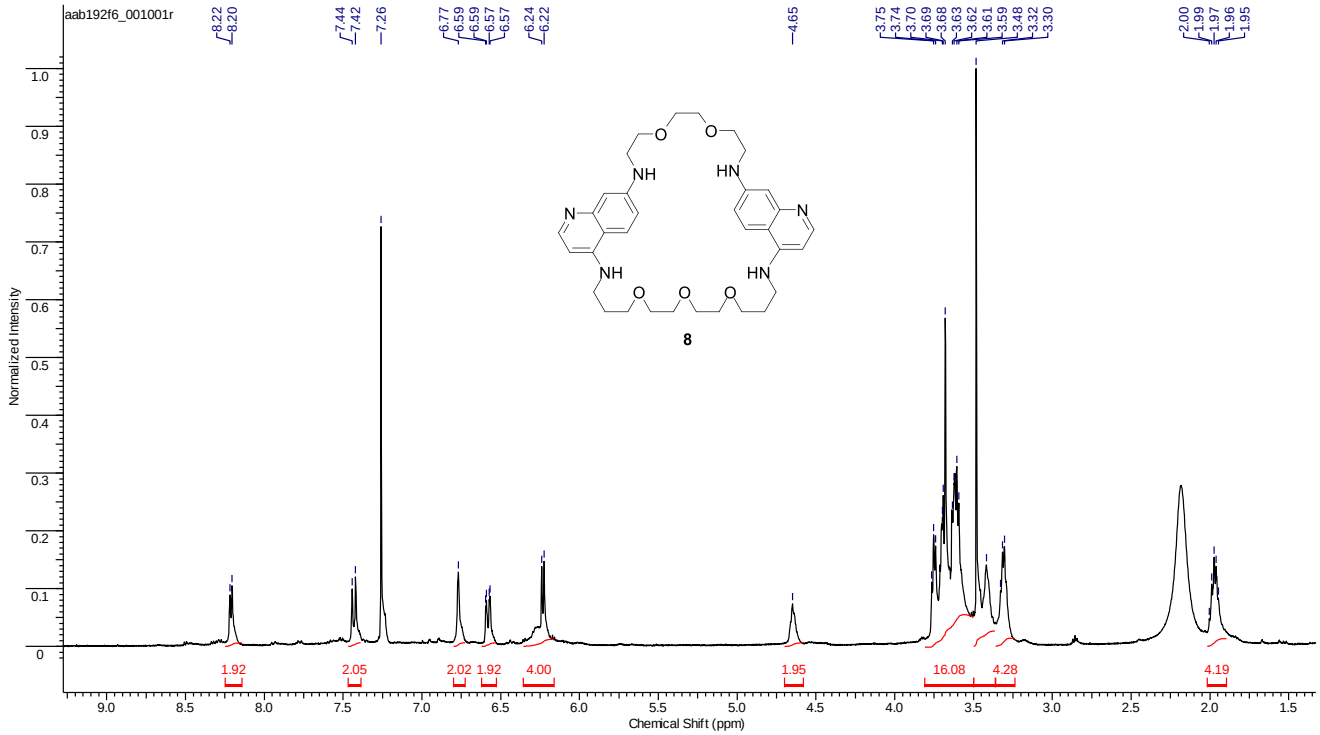


**Figure S49.** $^{1}$H NMR spectrum of **8** ($CDCl_3$, 400MHz, 300K).

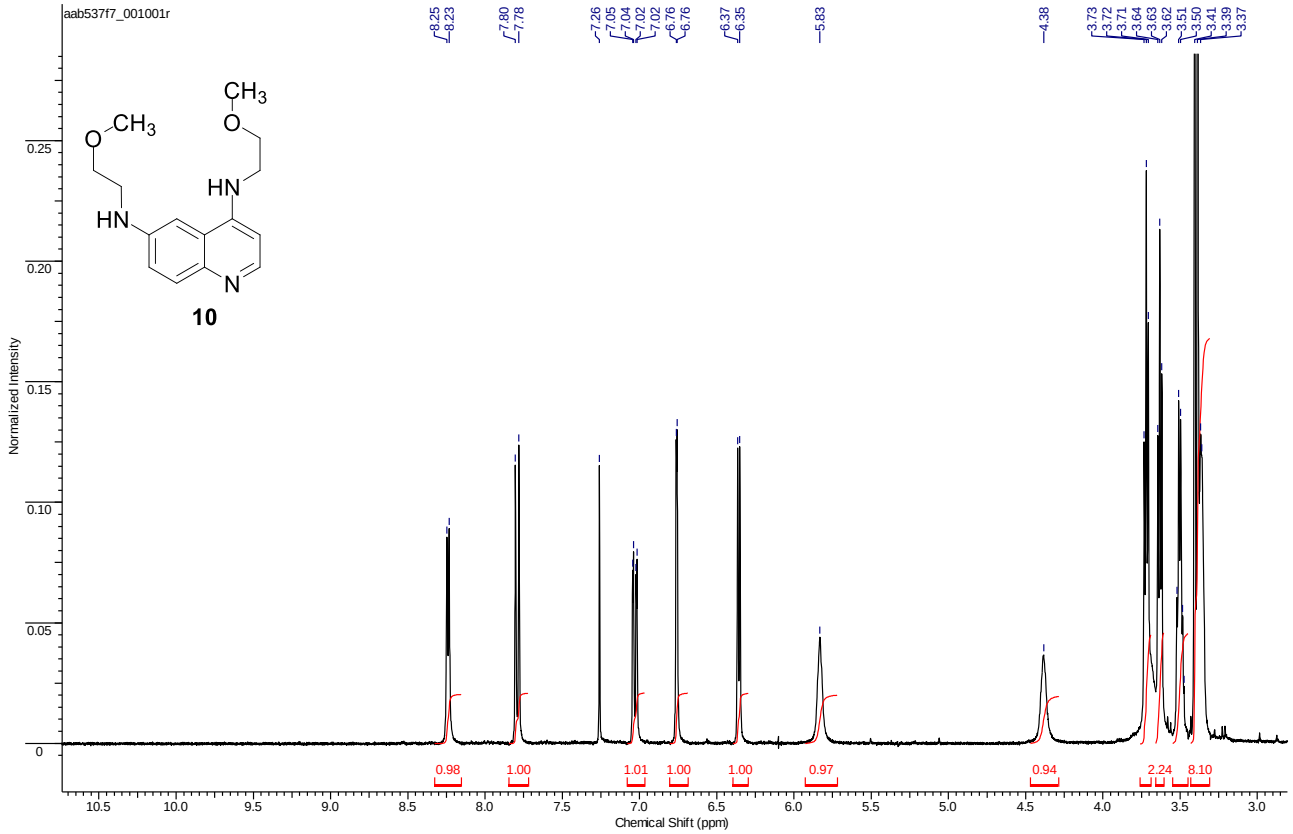


**Figure S50.** $^{1}$H NMR spectrum of **10** ($CDCl_3$, 400MHz, 300K).

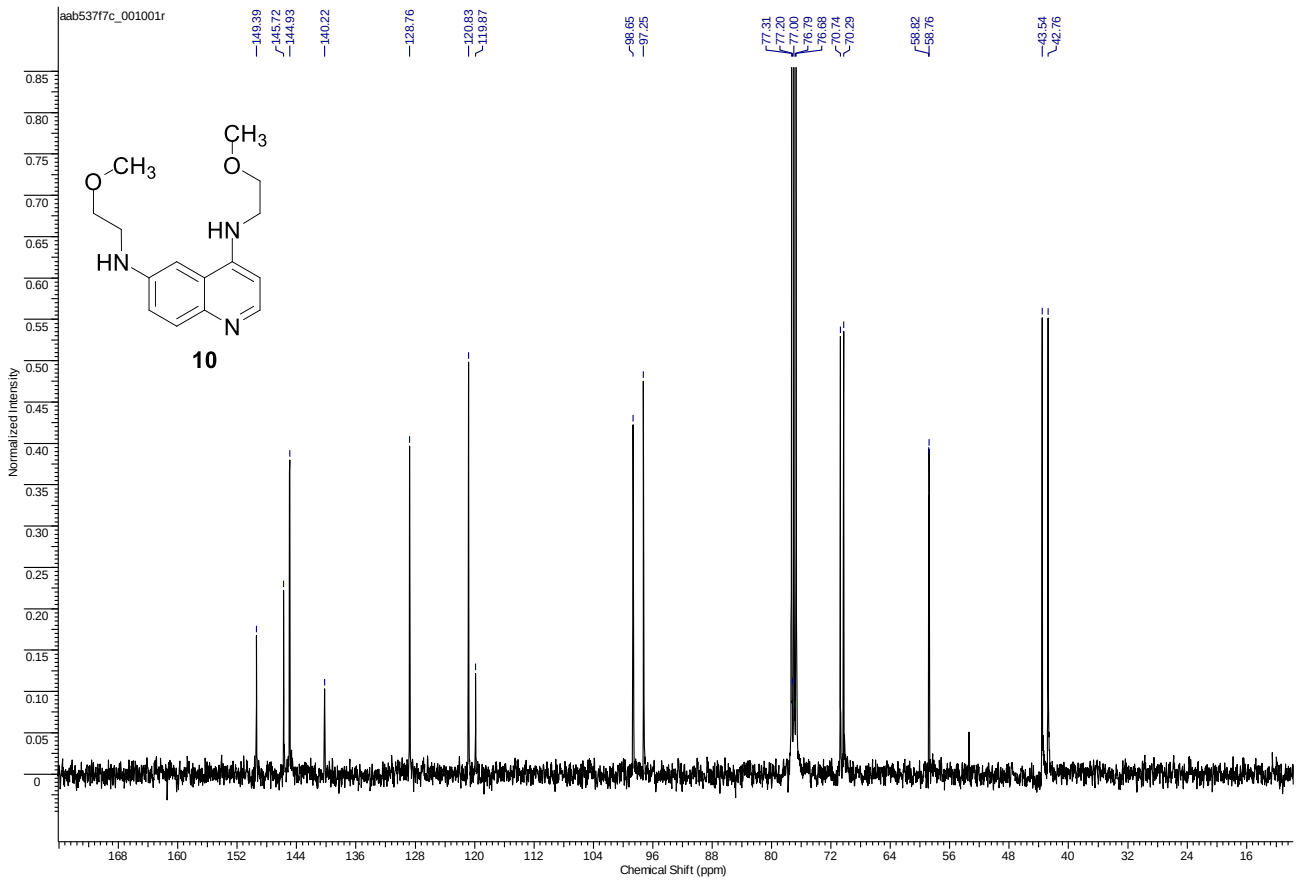


**Figure S51.** $^{13}$C NMR spectrum of **10** ($CDCl_3$, 400MHz, 300K).

## 7. References


1 R. A. Binstead, B. Jung, A. D. Zuverbühler, *SPECFIT/32, Global Analysis System, ver 3.0; Spectrum Software Associates: Marlborough, USA* **2000**.

2 P. MacCarthy, *Anal. Chem.*, **1978**, 50, 14, 2165.